Nuclear-structure theory in connection with neutrino physics

Jouni Suhonen

Department of Physics, University of Jyväskylä

MAYORANA International School, Modica, Sicily, July 4-11, 2023

Contents:

- Intro: Basics about weak decays
- Double beta decays and the g_A problem
- Effective value of g_A
- Electron spectral shapes and reactor $\bar{\nu}$
- Low Q values for $\nu/\bar{\nu}$ mass measurements
- Nuclear muon capture

Basics of neutrino-nucleus processes

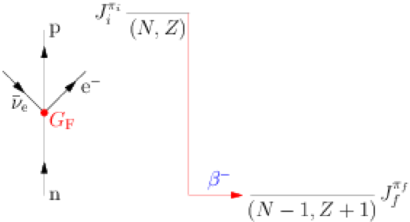

β^- decay: $\mathrm{n} \rightarrow \mathrm{p} + \mathrm{e}^- + \bar{\nu}_\mathrm{e}$

Decay rate

Driven by Q-value (= decay energy)

$Q = E_\mathrm{kin}(\mathrm{e}^-) + E_\mathrm{kin}(\bar{\nu})$

Hindered strongly by $\Delta J = |J_i - J_f|$ and very strongly by ${G_\mathrm{F}}^2$

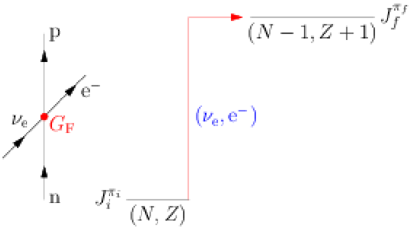

Neutrino-nucleus (charged-current) scattering at low energies ($<$ 100 MeV):

$\nu_\mathrm{e} + \mathrm{n} \rightarrow \mathrm{p} + \mathrm{e}^-$

Cross section

Driven by $E_\nu > E_\mathrm{threshold}$

Diminished moderately by $\Delta J = |J_i - J_f|$ and very strongly by ${G_\mathrm{F}}^2$

Examples:

β decays for isobars $A = 75$

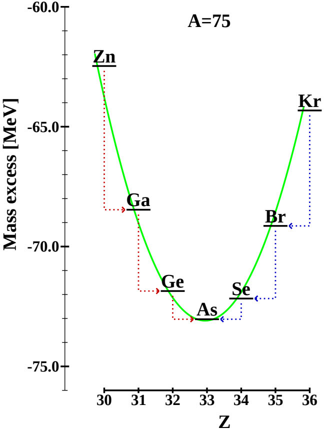

Charged-current scattering off ^{92}Mo

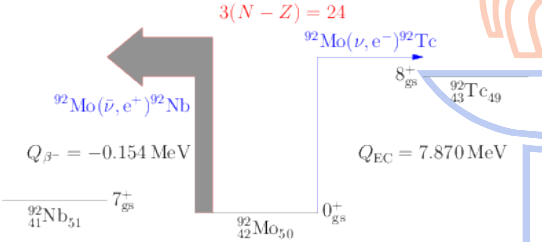

INTRO: Rare weak decays (of interest for determination of ν properties)

What causes the rare weak decays to be so rare?

- Very low decay energies (Q values) of β decays
- Weak-interaction processes of higher order ($\beta\beta$ decays)
- Large difference in the angular momenta of the initial and final states (forbidden β decays)

See the recent reviews:

H. Ejiri, J. S., K. Zuber: Neutrino-nuclear responses for astro-neutrinos, single beta decays and double beta decays, Physics Reports 797 (2019) 1–102

K. Blaum, S. Eliseev, F. A. Danevich, V. I. Tretyak, S. Kovalenko, M. I. Krivoruchenko, Yu. N. Novikov and J. S., Neutrinoless double-electron capture, Reviews of Modern Physics 92 (2020) 1–61.

Electron spectra and forbidden beta transitions

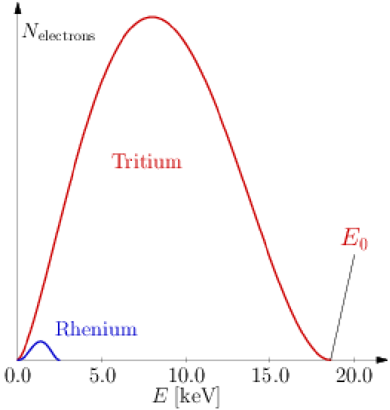

E = kinetic energy of the emitted electron

E_0 = endpoint energy

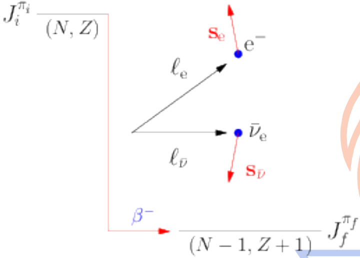

$$\mathbf{S} = \mathbf{s}_\mathrm{e} + \mathbf{s}_{\bar{\nu}} \; ; \mathbf{S} \leftrightarrow s = 0(\mathrm{F}), 1(\mathrm{GT})$$

$$\mathbf{L} = \mathbf{l}_\mathrm{e} + \mathbf{l}_{\bar{\nu}} \; ; \mathbf{L} \leftrightarrow \ell$$

$$\mathbf{J} = \mathbf{L} + \mathbf{S} \; ; \Delta(\mathbf{J}_i, \mathbf{J}, \mathbf{J}_f) \; ; \pi_i(-1)^\ell \pi_f = 1$$

Decay rate $\sim (\langle qr \rangle^2)^\ell \sim (10^{-4})^\ell$,

$$\mathbf{q} = \mathbf{p}_\mathrm{e} + \mathbf{p}_{\bar{\nu}}$$

$\ell = 0 \leftrightarrow$ allowed transition

$\ell \geq 1 \leftrightarrow$ ℓ:th forbidden transition

$|J_i - J_f| = \ell + 1 \leftrightarrow$ only one NME involved

$\leftrightarrow$ unique ℓ:th forbidden transition

Evaluation of the decay rates: allowed decays

$$\beta^- \text{ decay rate } = \frac{\ln 2}{T_{1/2}} =$$

$$G_{\rm F}\frac{m_{\rm e}^5c^4}{2\pi^3\hbar^7}\int_1^{w_0} C(w_{\rm e})p_{\rm e}w_{\rm e}(w_0-w_{\rm e})^2F_0(Z,w_{\rm e})dw_{\rm e} =$$

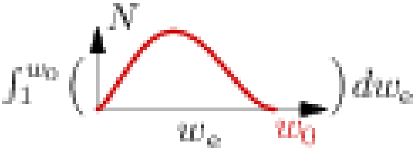

$C(w_{\rm e}) = g_{\rm V}{}^2M_{\rm F}^2 + g_{\rm A}{}^2M_{\rm GT}^2 \leftrightarrow$ shape factor for allowed decays

$w_{\rm e} = (E + m_{\rm e}c^2)/m_{\rm e}c^2 \leftrightarrow$ electron energy

$w_0 = (E_0 + m_{\rm e}c^2)/m_{\rm e}c^2 \leftrightarrow$ electron endpoint energy

$p_{\rm e} \leftrightarrow$ electron momentum

$F_0(Z, w_{\rm e}) \leftrightarrow$ Fermi function for final-state Coulomb effects

$g_{\rm V} = 1$ is the vector coupling (CVC value!)

$g_{\rm A}$ is the axial-vector coupling

Effective value of the weak axial coupling g_A

The PCVC hypothesis $\Rightarrow g_A = 1.27$

$\Downarrow$ Non-nucleonic degrees of freedom (delta resonances)

$\Downarrow$ Nuclear many-body effects (two-body currents)

$\Downarrow$ Nuclear-model effects (configuration-space truncations, neglect of three-nucleon forces,...)

Effective value: g_A^{eff}

Effective value of g_A affects everything

Motivation:

Effective value of the weak coupling g_A is involved in all weak processes, and thus have impact on

- studies of rare β decays
- processes in neutrino physics ($\beta\beta$ decay, low-energy (anti)neutrino-nucleus scattering, nuclear muon capture, . . .)
- processes in astrophysics (allowed and forbidden β decays, (anti)neutrino-nucleus scattering cross sections,. . .)

$\Downarrow$

Affects (strongly) the determination of neutrino properties!

Allowed Gamow-Teller decays

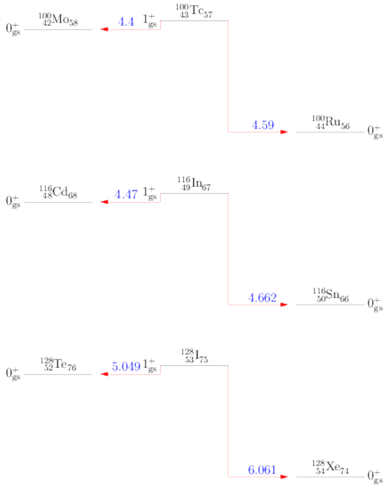

Try to determine $g_{\rm A}^{\rm eff}$ by reproducing experimental comparative half-lives (= $\log ft$ values) by the random-phase approximation theory

$$\log ft = \log(f_0 t_{1/2}[\mathrm{s}]) = \log\left(\frac{6289}{g_{\rm V}^2 M_{\rm F}^2 + {g_{\rm A}}^2 M_{\rm GT}^2}\right)$$

QUESTION: Can this be done?

Yes: Recent work by O. Civitarese, F. Deppisch, H. Ejiri, P. Pirinen, J. S.: quenched $g_{\rm A}^{\rm eff}$

Evaluation of the decay rates: unique forbidden decays (with universal spectral shape)

$$
\begin{aligned}
C_{lu}(w_e) &= (6.71 \times 10^{-6})^{l} \frac{(2l)!!}{(2l+1)!!} \\
&\times \left\{ \sum_{k_e+k_\nu=l+2} \frac{1}{\sqrt{(2k_e-1)!(k_\nu-1)!}} \frac{F_{k_e-1}(Z,w_e)}{F_0(Z,w_e)} \right. \\
&\times \left. p_e^{2(k_e-1)}(w_0-w_e)^{2(k_\nu-1)} \right\} \times {g_A}^2 {M_{lu}}^2
\end{aligned}
$$

$\leftrightarrow$ shape function for l:th forbidden unique decays

First-forbidden unique beta decays

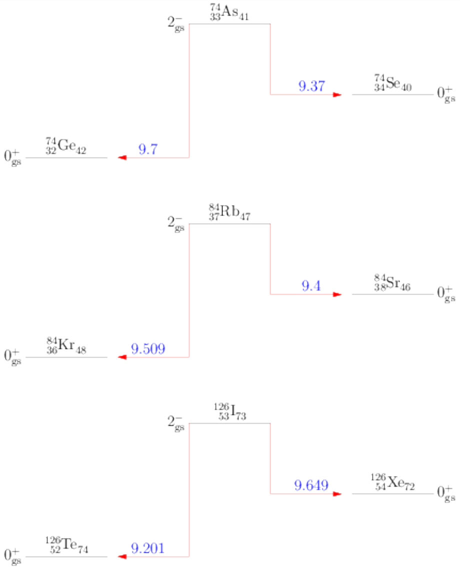

Extract $g_A^{\rm eff}$ by reproducing the $\log ft$ values of the beta decays.

⇓

QUESTION: Anything sensible coming out?

⇓

ANSWER: H. Ejiri, N. Soukouti and J. S., Phys. Lett. B 729 (2014) 27: quenched $g_A^{\rm eff}$

Decay rates, non-unique forbidden decays: $C(w_e)$

$$
\begin{aligned}
= & \frac{1}{\sqrt{2}}(6.71\times 10^{-6})^{l}\sqrt{\frac{(2l)!!}{(2l+1)!!}}\sum_{k_e+k_\nu=l+1}\frac{1}{\sqrt{(2k_e-1)!(2k_\nu-1)!}}\frac{F_{k_e-1}(Z,w_e)}{F_0(Z,w_e)}p_e^{2(k_e-1)}(w_0-w_e)^{2(k_\nu-1)}\\
\times & \left[\frac{2l+1}{l}\left(\frac{\hbar c}{m_ec^2}g_AM_1\right)^2+\frac{1}{(2k_e+1)^2}\left\{\left(\frac{\alpha\hbar c}{Rm_ec^2}Z\right)^2\left[g_VM_2^{(k_e)}-\sqrt{\frac{l+1}{l}}g_AM_3^{(k_e)}\right]^2\right.\right.\\
+ & 2\left(\frac{\alpha\hbar c}{Rm_ec^2}Z\right)w_e\left[g_VM_2-\sqrt{\frac{l+1}{l}}g_AM_3\right]\left[g_VM_2^{(k_e)}-\sqrt{\frac{l+1}{l}}g_AM_3^{(k_e)}\right]+(1+w_e^2)\left[g_VM_2-\sqrt{\frac{l+1}{l}}g_AM_3\right]^2\Bigg\}\\
- & \frac{2\sqrt{k_e^2-(\alpha Z)^2}}{k_ew_e(2k_e+1)^2}\left\{\frac{\alpha\hbar c}{Rm_ec^2}Z\left[g_VM_2-\sqrt{\frac{l+1}{l}}g_AM_3\right]\left[g_VM_2^{(k_e)}-\sqrt{\frac{l+1}{l}}g_AM_3^{(k_e)}\right]\right.\\
+ & w_e\left[g_VM_2-\sqrt{\frac{l+1}{l}}g_AM_3\right]^2\Bigg\}+\frac{1}{(2k_\nu+1)^2}(w_0-w_e)^2\left[g_VM_2+\sqrt{\frac{l+1}{l}}g_AM_3\right]^2-\frac{2}{2k_e+1}\sqrt{\frac{2l+1}{l}}\\
\times & \left\{\left(\frac{\alpha\hbar c}{Rm_ec^2}Z\right)\left(\frac{\hbar c}{m_ec^2}g_AM_1\right)\left[g_VM_2^{(k_e)}-\sqrt{\frac{l+1}{l}}g_AM_3^{(k_e)}\right]+w_e\left(\frac{\hbar c}{m_ec^2}g_AM_1\right)\left[g_VM_2-\sqrt{\frac{l+1}{l}}g_AM_3\right]\right\}\\
+ & \frac{2}{2k_e+1}\sqrt{\frac{2l+1}{l}}\frac{\sqrt{k_e^2-(\alpha Z)^2}}{k_ew_e}\left(\frac{\hbar c}{m_ec^2}g_AM_1\right)\left[g_VM_2-\sqrt{\frac{l+1}{l}}g_AM_3\right]-\frac{2}{2k_\nu+1}\sqrt{\frac{2l+1}{l}}(w_0-w_e)\\
\times & \left(\frac{\hbar c}{m_ec^2}g_AM_1\right)\left[g_VM_2+\sqrt{\frac{l+1}{l}}g_AM_3\right]+\frac{2}{(2k_e+1)(2k_\nu+1)}(w_0-w_e)\left\{\left(\frac{\alpha\hbar c}{Rm_ec^2}Z\right)\right.\\
\times & \left.\left.\left[g_VM_2^{(k_e)}-\sqrt{\frac{l+1}{l}}g_AM_3^{(k_e)}\right]+w_e\left[g_VM_2-\sqrt{\frac{l+1}{l}}g_AM_3\right]\right\}\left[g_VM_2+\sqrt{\frac{l+1}{l}}g_AM_3\right]\right]
\end{aligned}
$$

non-unique forbidden decays continues...

$$
\begin{aligned}
- \quad & \frac{2}{(2k_e+1)(2k_\nu+1)} \frac{\sqrt{k_e^2-(\alpha Z)^2}}{k_e w_e}(w_0-w_e)\left[g_V M_2 - \sqrt{\frac{l+1}{l}} g_A M_3\right]\left[g_V M_2 + \sqrt{\frac{l+1}{l}} g_A M_3\right]\Bigg] \\
+ \quad & (6.71\times 10^{-6})^l \sqrt{\frac{(2l)!!}{(2l+1)!!}} \sum_{k_e+k_\nu=l+2} \frac{1}{\sqrt{(2k_e-1)!(2k_\nu-1)!}} \frac{F_{k_e-1}(Z,w_e)}{F_0(Z,w_e)} p_e^{2(k_e-1)} (w_0-w_e)^{2(k_\nu-1)} \\
\times \quad & \left[\frac{(l+1)}{(2k_e-1)(2k_\nu-1)}\left\{ {g_V}^2 {M_2}^2 + 2 g_V g_A \frac{k_e-k_\nu}{\sqrt{l(l+1)}} M_2 M_3 + \frac{(k_e-k_\nu)^2}{l(l+1)} {g_A}^2 {M_3}^2 \right\} + {g_A}^2 {M_4}^2 \right]
\end{aligned}
$$

$\leftrightarrow$ shape function for forbidden non-unique decays

Extension to include also the next-order terms: M. Haaranen, J. Kotila and J. S., Phys. Rev. C 95 (2017) 024327.

Motivation for the Work: Double Beta Decay

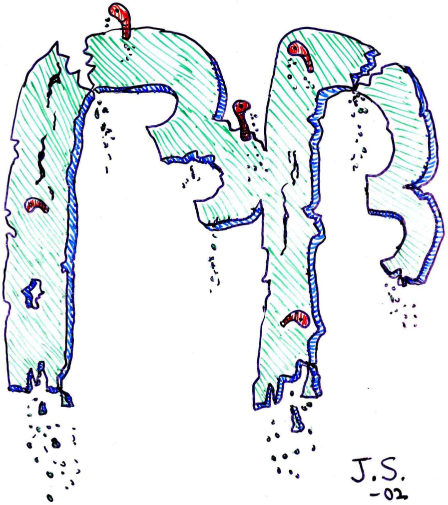

Highly-suppressed weak decays

Nuclear decays of higher order:

Double beta decays:

Two-neutrino $\beta\beta$ decay

and

NEUTRINOLESS $\beta\beta$ decay

$2\nu\beta\beta$ decay from nuclear-structure point of view

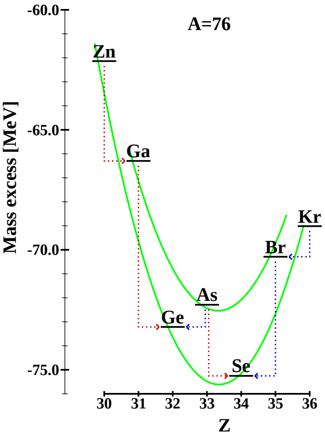

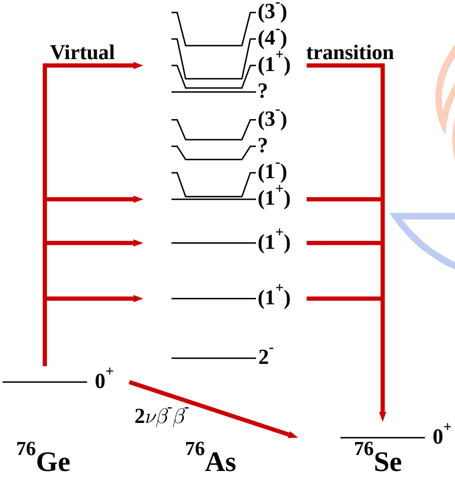

Two-neutrino double beta decay

Nucleus	half-life (years)	experiments
^{48}Ca	$4.4^{+0.6}_{-0.5} \cdot 10^{19}$	laboratory
^{76}Ge	$1.60^{+0.13}_{-0.10} \cdot 10^{21}$	laboratory
^{82}Se	$(0.92 \pm 0.07) \cdot 10^{19}$	laboratory, geochemical
^{96}Zr	$(2.3 \pm 0.2) \cdot 10^{19}$	laboratory, geochemical
^{100}Mo	$(7.1 \pm 0.4) \cdot 10^{18}$	laboratory
^{100}Mo(0^+_1)	$6.2^{+0.7}_{-0.5} \cdot 10^{20}$	laboratory
^{116}Cd	$(2.85 \pm 0.15) \cdot 10^{19}$	laboratory
^{128}Te	$(2.0 \pm 0.3) \cdot 10^{24}$	geochemical
^{130}Te	$(6.9 \pm 1.3 \cdot 10^{20}$	geochemical
^{136}Xe	$(2.20 \pm 0.06) \cdot 10^{21}$	laboratory
^{150}Nd	$(8.2 \pm 0.9) \cdot 10^{18}$	laboratory
^{150}Nd(0^+_1)	$1.33^{+0.45}_{-0.26} \cdot 10^{20}$	laboratory
^{238}U	$(2.0 \pm 0.6) \cdot 10^{21}$	radio-chemical

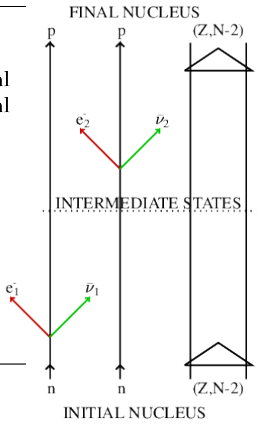

10^{20} years $=$
$10000000000 \times$ age of the UNIVERSE

Convergence of the large-scale shell-model calculation in the single-particle model space $0f_{5/5} - 1p - 0g_{9/2}$ using the effective Hamiltonian JUN45 (M. Honma *et al.*, Phys. Rev. C 80 (2009) 064323)

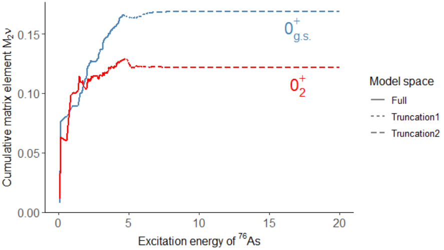

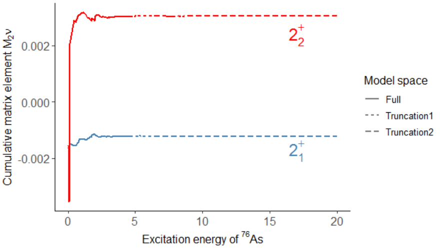

$2\nu\beta\beta$ decay of ^{76}Ge: Relative feeding of final states

J. Kostensalo, J.S, K. Zuber, Phys. Lett. B 831 (2022) 137170

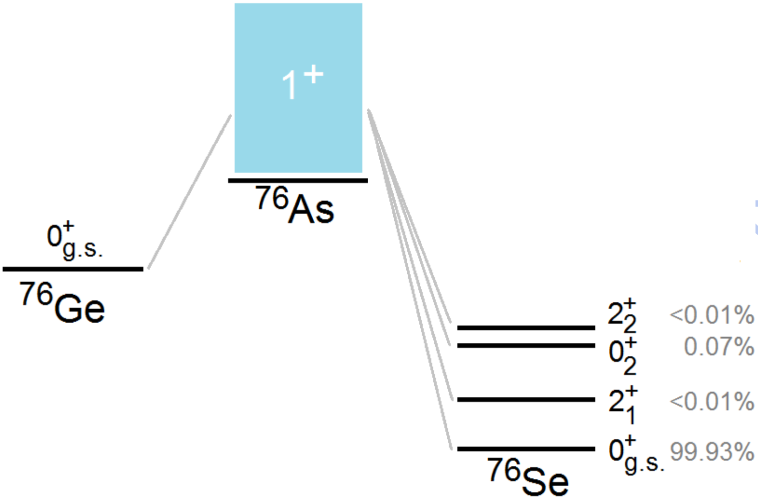

^{96}Zr and ^{48}Ca: Competition of beta and double beta decays

^{48}Ca decay channels calculated by the SHELL MODEL

M. Haaranen, M. Horoi, J.S, Phys. Rev. C 89 (2014) 034315

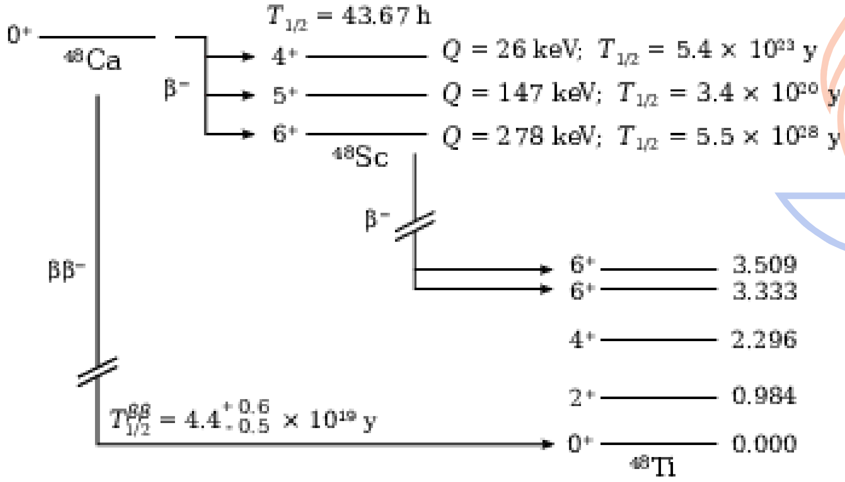

^{96}Zr decay channels calculated by the pnQRPA

H. Heiskanen, M. T. Mustonen, J.S, J. Phys. G 34 (2007) 837

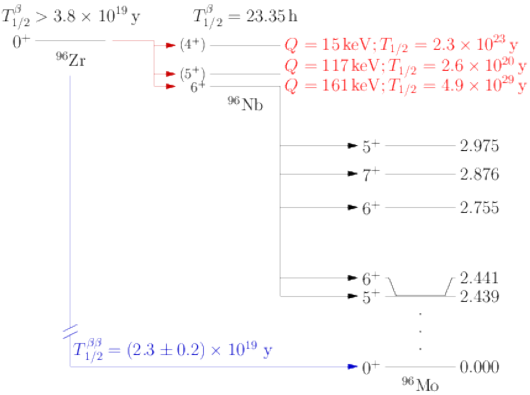

$0^+ \rightarrow 4^+ \leftrightarrow$ 4th forbidden non-unique transition

$0^+ \rightarrow 5^+ \leftrightarrow$ 4th forbidden unique transition

$0^+ \rightarrow 6^+ \leftrightarrow$ 6th forbidden non-unique transition

Neutrinoless double β^- decay

$0\nu\beta\beta$ Decay is Able to:

- Reveal if the neutrino is a Majorana particle
- Probe the neutrino effective mass $\langle m_\nu \rangle = \sum_{j=\text{light}} \lambda_j^{\text{CP}} |U_{ej}|^2 m_j$
- Probe the degenerate or inverted mass hierarchies (next-generation experiments!)
- Probe possibly the CP phases (nuclear matrix elements are critical!)

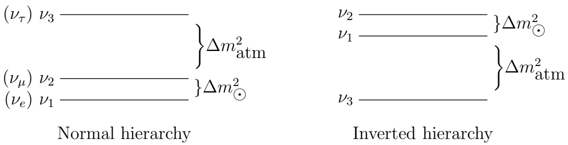

$$\Delta m^2_\odot = 7.67^{+0.16}_{-0.19} \times 10^{-5}\,\text{eV}^2$$
$$\Delta m^2_{\text{atm}} = 2.39^{+0.11}_{-0.08} \times 10^{-3}\,\text{eV}^2$$

[Global 3ν oscillation analysis (2008)]

MASS MODE:
$T_{1/2}^{-1} \propto \langle m_\nu \rangle^2$

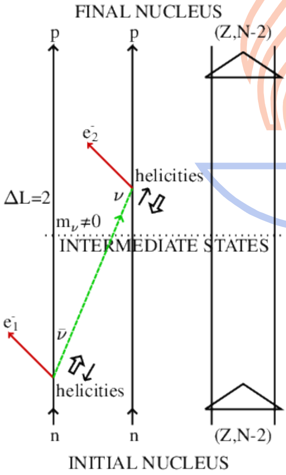

$0\nu\beta\beta$ decay from nuclear-structure point of view

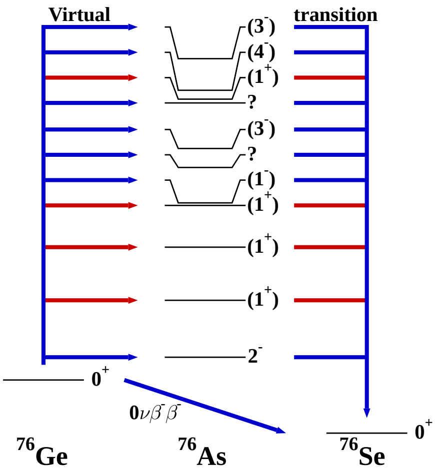

Decay rate:

$$\frac{\ln 2}{T_{1/2}} = (g_{\rm A})^4 g^{(0\nu)}(Q)[M^{(0\nu)}]^2 \langle m_\nu \rangle^2$$

- $g^{(0\nu)}(Q) \propto Q^5$ is the phase-space factor
- $M^{(0\nu)}$ = NUCLEAR MATRIX ELEMENT
- Effective neutrino mass:

$$\langle m_\nu \rangle = \sum_{j={\rm light}} \lambda_j^{\rm CP} |U_{{\rm e}j}|^2 m_j$$

- Light and heavy Majorana-neutrino exchange: J. Hyvärinen and J.S., Phys. Rev. C 91 (2015) 024613

INTRO: The Standard Model

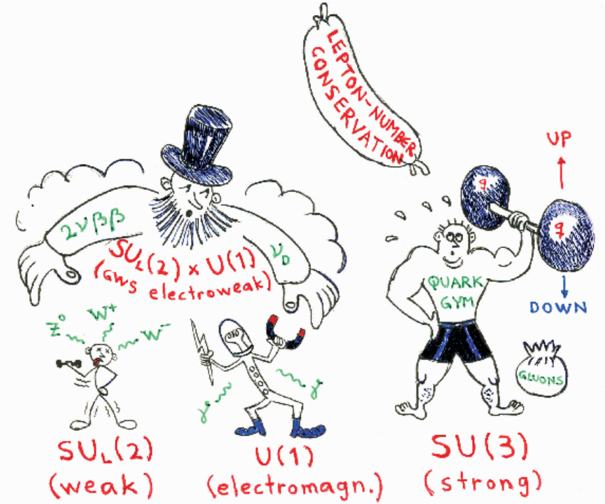

- Only massless neutrinos
- Only Dirac neutrinos
- Lepton number is conserved

Example of a Theory Containing Massive Neutrinos

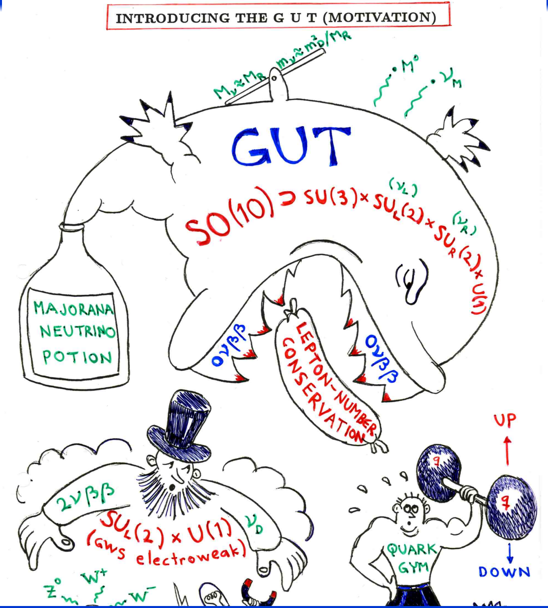

SPECIFIC FEATURES OF $0\nu\beta^-\beta^-$ DECAYS

Matrix Elements of the $0\nu\beta^-\beta^-$ Decay

MASS MODE:

$$\left[T_{1/2}^{(0\nu)}\right]^{-1} = (g_{\rm A})^4 G^{(0\nu)} \left(\frac{\langle m_\nu \rangle}{m_{\rm e}}\right)^2 |M^{(0\nu)}|^2 ,$$

$$M^{(0\nu)} = M_{\rm GT}^{(0\nu)} - \left(\frac{g_{\rm V}}{g_{\rm A}}\right)^2 M_{\rm F}^{(0\nu)} + M_{\rm T}^{(0\nu)} ,$$

$$G_1^{(0\nu)}(Q) \propto Q^5 \text{ is the phase-space factor } ,$$

$$\langle m_\nu \rangle = \sum_j \lambda_j^{\rm CP} m_j |U_{{\rm e}j}|^2 (\text{Effective neutrino mass}) ,$$

$$M_{\rm F}^{(0\nu)} = \sum_a (0_f^+ || \sum_{mn} h_+(r_{mn}, E_a) || 0_i^+) ,$$

$$M_{\rm GT}^{(0\nu)} = \sum_a (0_f^+ || \sum_{mn} h_+(r_{mn}, E_a)(\boldsymbol{\sigma}_m \cdot \boldsymbol{\sigma}_n) || 0_i^+) .$$

Specific Properties of $0\nu\beta^-\beta^-$ NMEs

Nucleon-nucleon short-range correlations:

one has to prevent the two
decaying nucleons to overlap

$\longrightarrow$ Use a short-range correlator, like Jastrow (traditional) or **UCOM** (applied already in 2007 by the Jyväskylä group)

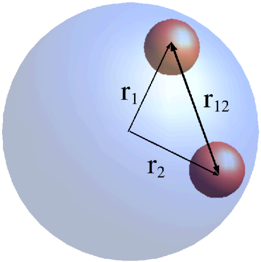

Other improvements (Tübingen, 1999):

finite nucleon size (form factors)
and
higher-order terms in nucleonic weak current

Nucleonic Weak Current and Nucleon Form Factors

Lepton-nucleon weak current:

$$H_W = \frac{G_F}{\sqrt{2}} \left(j_{L\mu} J_L^{\mu\dagger} \right) + \text{H.c.} \quad ; \quad j_{L\mu} = \bar{e}\gamma_\mu(1-\gamma_5)\nu_{eL} \ ,$$

$$J_L^{\mu\dagger} \approx \bar{\Psi}\tau^+ \left[g_V(\mathbf{q}^2)\gamma^\mu - i g_M(\mathbf{q}^2)\frac{\sigma^{\mu\nu}}{2M_N}q_\nu - g_A(\mathbf{q}^2)\gamma^\mu\gamma_5 + g_P(\mathbf{q}^2)q^\mu\gamma_5 \right] \Psi$$

Ψ = nucleon fields, M_N = nucleon mass, $\sigma^{\mu\nu} = \frac{i}{2}[\gamma^\mu, \gamma^\nu]$

The dipole form factors read:

$$g_V(\mathbf{q}^2) = \frac{g_V}{(1+\mathbf{q}^2/M_V^2)^2} \ ; \ g_A(\mathbf{q}^2) = \frac{g_A}{(1+\mathbf{q}^2/M_A^2)^2} \ ,$$

$g_V = 1.00$, $g_A =$ **???**, $M_V = 850\,\text{MeV}, M_A = 1086\,\text{MeV}$,
$g_M(\mathbf{q}^2) = (\mu_p - \mu_n) g_V(\mathbf{q}^2)$ [Weak magnetism]
$g_P(\mathbf{q}^2) = 2M_N g_A(\mathbf{q}^2)(\mathbf{q}^2 + m_\pi^2)^{-1}$ [Goldberger-Treiman relation]

About the Nuclear Models

Nuclear Models:

HOW CAN WE DESCRIBE THE VIRTUAL TRANSITIONS?

Single-particle space

particle creation: $c_p^\dagger, c_n^\dagger$
(p = proton, n = neutron)

$\Downarrow$ BCS

Quasiparticle mean field

quasiparticle creation: $a_p^\dagger, a_n^\dagger$

$\Downarrow$ pnQRPA

Basic excitation:

$$\Gamma_{kJ}^\dagger = \sum_{pn} \left(X_{pn}^k \left[a_p^\dagger a_n^\dagger\right]_J - Y_{pn}^k \left[a_p^\dagger a_n^\dagger\right]_J^\dagger \right)$$

$\Downarrow$

We bosonize

$$[H, \Gamma_{kj}^\dagger]|0\rangle = E_k \Gamma_{kj}^\dagger |0\rangle$$

$\Downarrow$

Equations of motion

$$\begin{pmatrix} A(g_{\rm ph}, g_{\rm pp}) & B(g_{\rm ph}, g_{\rm pp}) \\ -B(g_{\rm ph}, g_{\rm pp})^* & -A(g_{\rm ph}, g_{\rm pp})^* \end{pmatrix} \begin{pmatrix} X^k \\ Y^k \end{pmatrix} = E_k \begin{pmatrix} X^k \\ Y^k \end{pmatrix}$$

Determination of the Values of the Scaling Parameters

- Value of $g_{\rm ph} \longleftrightarrow$ Energy centroid of the GTGR (Gamow–Teller giant resonance)
- $g_{\rm pp}$ remains a free parameter $\longleftrightarrow$ The "$g_{\rm pp}$ problem"

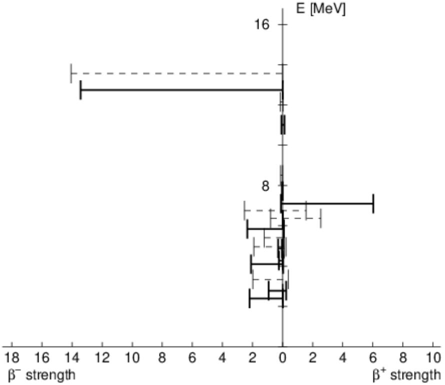

Calculated β^- and β^+ strengths for Gamow–Teller transitions from the pnQRPA ground state of ^{66}Zn to the 1^+ pnQRPA states in ^{66}Ga and ^{66}Cu. The dashed bars represent a 0f-1p calculation and the solid bars a 0f-1p-0$g_{9/2}$ calculation. (Jouni Suhonen, *From Nucleons to Nucleus*, Springer 2007)

Determination of the Value of the $g_{\rm pp}$ Parameter

$$M^{(0\nu)}_{\rm GT} = \sum_{J^\pi} M^{(0\nu)}_{\rm GT}(J^\pi) ,$$

$$M^{(0\nu)}_{\rm GT}(J^\pi) = \sum_{n\lambda} (0^+_f \| \sum_j [\boldsymbol{\sigma}_j F_\lambda(\mathbf{r}_j)]_J t^-_j \| J^\pi{}_n)$$
$$\times (J^\pi{}_n \| \sum_j [\boldsymbol{\sigma}_j F_\lambda(\mathbf{r}_j)]_J t^-_j \| 0^+_i)$$

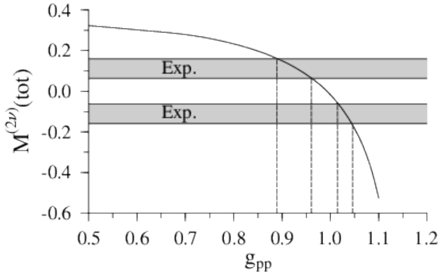

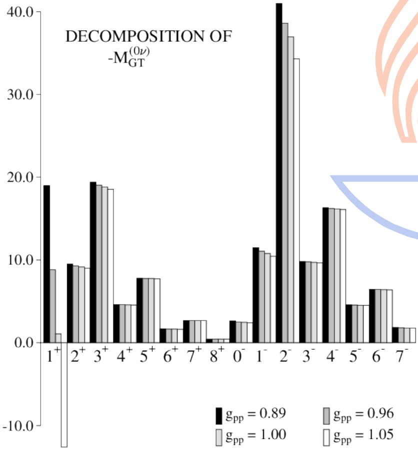

Interacting Shell Model (ISM) vs. pnQRPA

ISM

- Advantage: All configurations taken into account in a given single-particle space, e.g. the $0f_{5/2}$-$1p_{3/2}$-$1p_{1/2}$ space:

$$(\pi 0f_{5/2})^{x_p}(\pi 1p_{3/2})^{y_p}(\pi 1p_{1/2})^{Z_{\rm act}-x_p-y_p}$$
$$\times(\nu 0f_{5/2})^{x_n}(\nu 1p_{3/2})^{y_n}(\nu 1p_{1/2})^{N_{\rm act}-x_n-y_n}$$

- Disadvantage: Only small single-particle spaces possible due to computational reasons

pnQRPA

- Advantage: Large single-particle spaces computationally possible
- Disadvantage: Contains only a limited class of (quasiparticle) configurations in a given single-particle space, e.g.

$$A \times 2\text{qp} + B \times 6\text{qp} + C \times 10\text{qp} + \ldots ,$$

where A, B, C, ... are fixed by the form of the (correlated) pnQRPA ground state

Relevance of the Spin-Orbit-Partner Orbitals

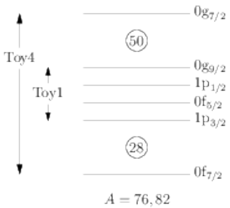

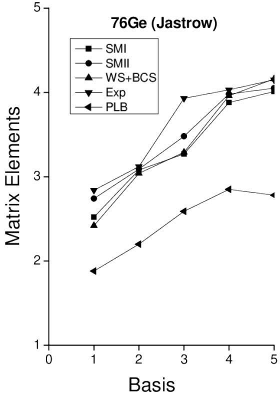

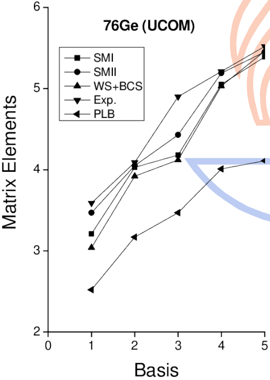

About $0\nu\beta\beta$-decay experiments

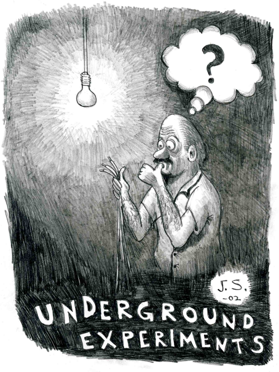

UNDERGROUND
LABORATORIES
protect from
COSMIC RAYS
and their secondary
particles

Canfranc (Spain)
Kamioka (Japan)
Boulby (England)
Gran Sasso (Italy)
Pyhäsalmi (Finland)
Baksan (Ukraine)
Modane (France-Italy)
Sudbury (Canada)

Experimental status (outdated)

Table: Presently running experiments with results.

Nucleus	Half-life (yr)	Experiment	$\langle m_\nu \rangle$ (eV)
^{76}Ge	$> 2.1 \cdot 10^{25}$	GERDA	$< 0.21 - 0.38$
^{82}Se	$> 3.6 \cdot 10^{23}$	NEMO-3	$< 0.89 - 1.61$
^{100}Mo	$> 1.1 \cdot 10^{24}$	NEMO-3	$< 0.29 - 0.93$
^{116}Cd	$> 1.7 \cdot 10^{23}$	SOLOTVINO	$< 1.17 - 2.76$
^{130}Te	$> 2.8 \cdot 10^{24}$	CUORICINO	$< 0.28 - 0.59$
^{136}Xe	$> 4.5 \cdot 10^{23}$	DAMA	$< 0.84 - 2.67$

Table: Prospects for the running and planned experiments.

Nucleus	Experiment	Mass (kg)	Sensitivity half-life (yr)	Sensitivity $\langle m_\nu \rangle$ (meV)	Status
^{76}Ge	MAJORANA I	$30 - 60$	$(1 - 2) \cdot 10^{26}$	$70 - 300$	In progress
	MAJORANA II	1000	$6 \cdot 10^{27}$	$10 - 40$	R&D
^{76}Ge	GERDA I	40	$2 \cdot 10^{26}$	$70 - 300$	In progress
	GERDA II	1000	$6 \cdot 10^{27}$	$10 - 40$	R&D
^{82}Se	SuperNEMO	$100 - 200$	$(1 - 2) \cdot 10^{26}$	$40 - 110$ R&D	
^{130}Te	CUORE	200	$2.1 \cdot 10^{26}$	$35 - 90$	In progress
^{136}Xe	EXO I	200	$6.4 \cdot 10^{25}$	$70 - 220$	Started in 2011
	EXO II	1000	$8 \cdot 10^{26}$	$20 - 65$	R&D
^{136}Xe	KamLAND-Zen I	400	$4.5 \cdot 10^{26}$	$30 - 95$	Started in 2011
	KamLAND-Zen II	1000	$\approx 10^{27}$	$20 - 65$	R&D
^{150}Nd	SNO+ I	56	$4.5 \cdot 10^{24}$	$130 - 300$	In progress
	SNO+ II	500	$3 \cdot 10^{25}$	$55 - 120$	R&D

Personal reminiscences

Inauguration Day of NEMO3, 12 July 2002

The ZORRO Experiment

Needs 100 kg of ^{96}Zr, this is a
PROBLEM

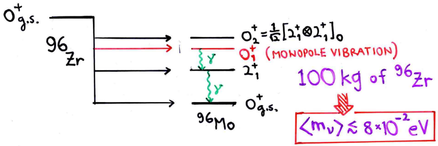

Double beta decays on the positron-emitting/electron-capture side

Double positron/EC decays (2ν decays have two ν_e in final state)

$0\nu\beta^+\beta^+$ Decay

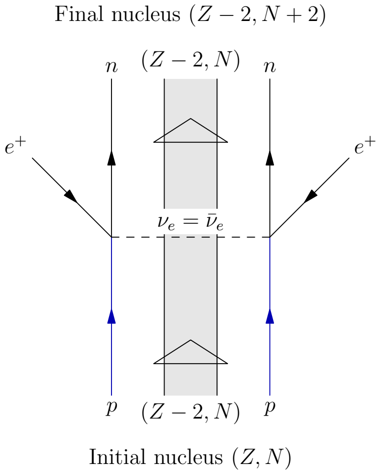

$0\nu\beta^+$EC Decay

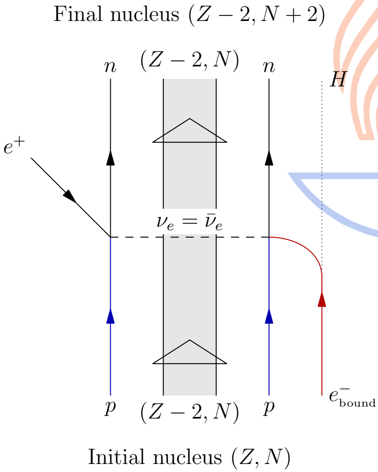

Two-neutrino double electron capture

Final nucleus $(Z-2, N+2)$

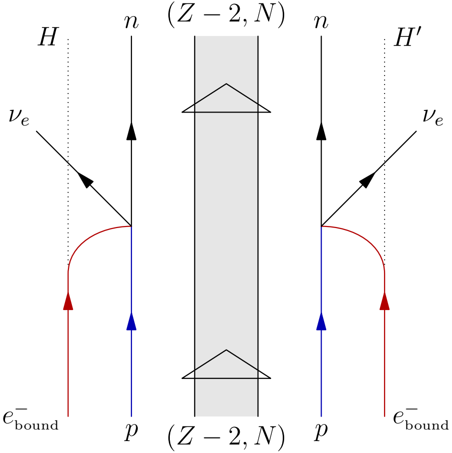

Initial nucleus (Z, N)

Example: Various $2\nu2\beta$ decay modes of ^{96}Ru (calculated by using pnQRPA)

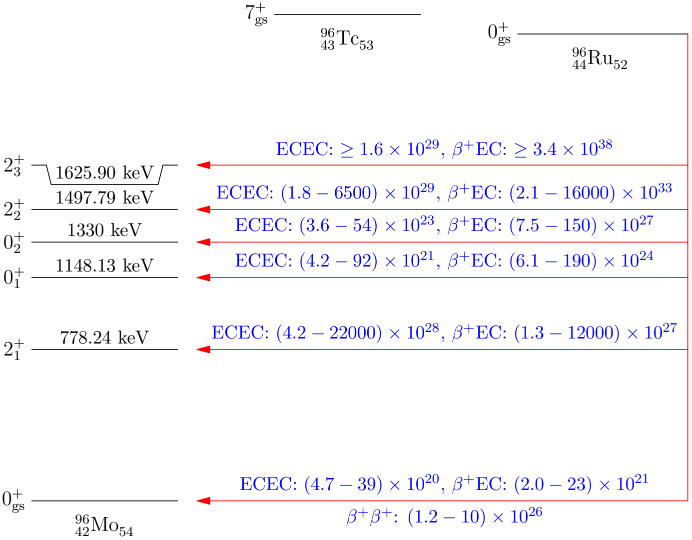

Example: Various $0\nu 2\beta$ decay modes of ^{78}Kr (calculated by using pnQRPA)

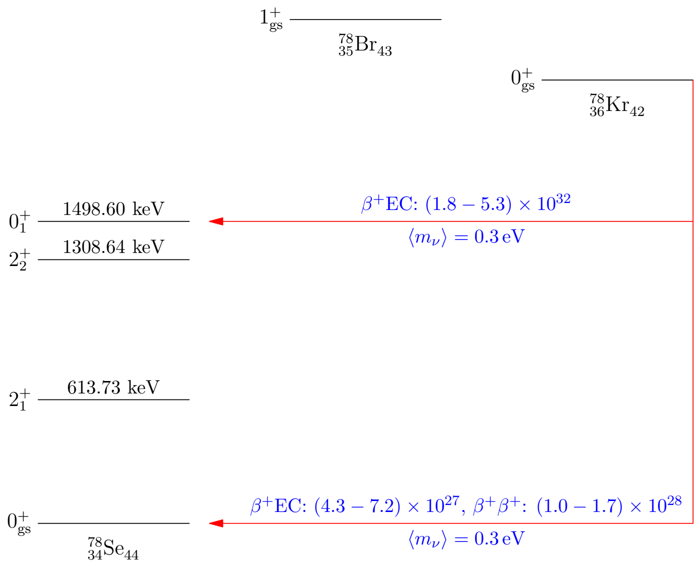

Neutrinoless double electron capture

Radiative 0νECEC

Final nucleus $(Z-2, N+2)$

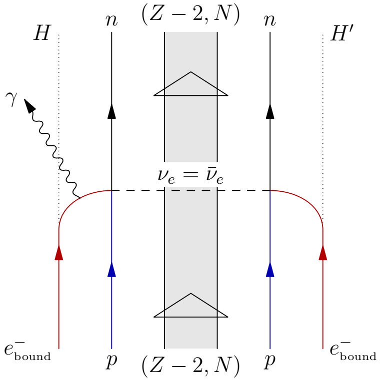

Initial nucleus (Z, N)

Resonant 0νECEC

Final nucleus $(Z-2, N+2)^*$

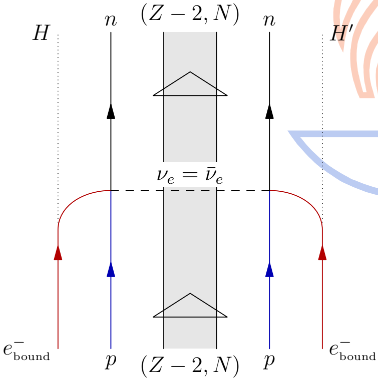

Initial nucleus (Z, N)

Rate of resonant 0νECEC Decay

$$\frac{\ln 2}{T_{1/2}} = g^{\mathrm{ECEC}}[M^{\mathrm{ECEC}}]^2 \frac{\langle m_\nu \rangle^2 \Gamma}{(Q-E)^2 + \Gamma^2/4} , \quad Q-E = \text{ degeneracy parameter}$$

- Atomic factor

$$g^{\mathrm{ECEC}}(0^+) = \left(\frac{G_{\mathrm{F}} \cos\theta_{\mathrm{C}}}{\sqrt{2}}\right)^4 \frac{(g_{\mathrm{A}})^4}{4\pi^2} m_{\mathrm{e}}^6 \mathcal{N}_{0,-1}^2 ,$$

  where $\mathcal{N}_{0,-1}$ is the normalization of the relativistic K-shell($1s_{1/2}$) Dirac wave function for a uniformly charged spherical nucleus
- $Q = M(Z,A) - M(Z-2,A) =$ difference between the initial and final atomic masses
- $E = E^* + E_H + E_{H'} + E_{HH'} =$ nuclear excitation energy + electron binding
- $\Gamma = \Gamma^* + \Gamma_H + \Gamma_{H'} =$ nuclear and atomic radiative widths
- NUCLEAR MATRIX ELEMENT: $M^{\mathrm{ECEC}} = \frac{1}{R_A} M^{(0\nu)'}$, $R_A = 1.2A^{1/3}$ fm

Enhancement factors of 10^6 possible (J. Bernabeu, A. De Rujula, and C. Jarlskog, Nucl. Phys. B 223 (1983) 15 ; Z. Sujkowski and S. Wycech, Phys. Rev. C 70 (2004) 052501(R))

Example: Various $2\nu2\beta$ decay modes of ^{124}Xe (calculated by using pnQRPA)

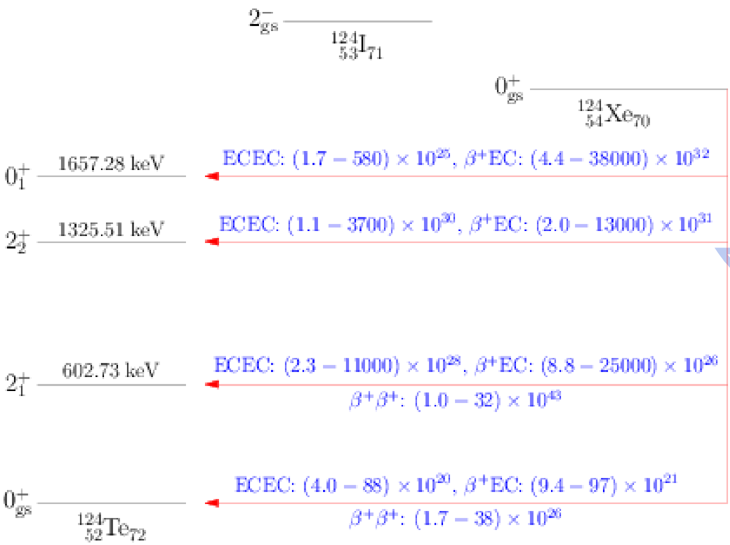

Example: Various $0\nu2\beta$ decay modes of ^{124}Xe (calculated by using pnQRPA)

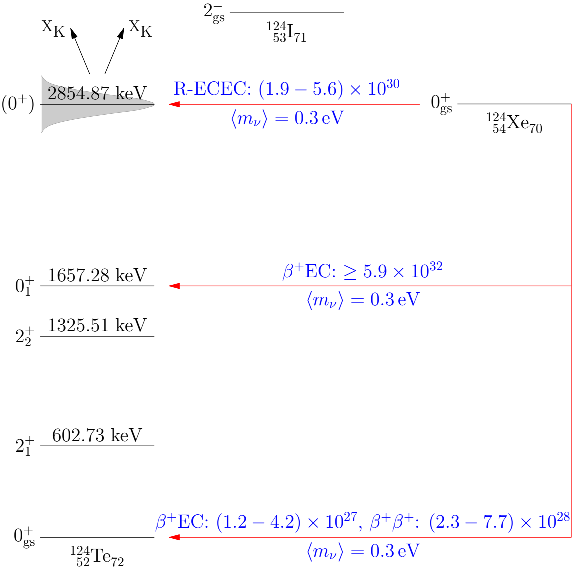

Concise List of Other Cases ($\langle m_\nu \rangle = 0.3\,\text{eV}$) Part I

Transition	J_f^π	$Q - E$ [keV]	At. orb.	$T_{1/2}$ [yr]	Ref.
$^{74}\text{Se} \rightarrow {}^{74}\text{Ge}$	2^+	2.23	L_2L_3	$(0.2 - 100) \times 10^{44}$	[1]
$^{96}\text{Ru} \rightarrow {}^{96}\text{Mo}$	2^+	8.92(13)	L_1L_3		[2]
	$0^+?$	$-3.90(13)$	L_1L_1	$(4.9 - 22) \times 10^{32}$	[3], Q [2]
$^{102}\text{Pd} \rightarrow {}^{102}\text{Ru}$	2^+	75.26(36)	KL_3		[4]
$^{106}\text{Cd} \rightarrow {}^{106}\text{Pd}$	$0^+?$	8.39	KK	$(2.3 - 6.3) \times 10^{31}$	[5], Q [4]
	$(2,3)^-?$	$-0.33(41)$	KL_3		[4]
$^{112}\text{Sn} \rightarrow {}^{112}\text{Cd}$	0^+	-4.5	KK	$> 6.6 \times 10^{30}$	[6]
$^{124}\text{Xe} \rightarrow {}^{124}\text{Te}$	$0^+?$	1.86(15)	KK	$(1.9 - 5.6) \times 10^{30}$	[7], Q [8]
$^{130}\text{Ba} \rightarrow {}^{130}\text{Xe}$	$0^+?$	10.18(30)	KK		[8]
$^{136}\text{Ce} \rightarrow {}^{136}\text{Ba}$	0^+	-11.67	KK	$(3.3 - 26) \times 10^{33}$	[9]

[1] V. Kolhinen *et al.*, PLB 684 (2010) 17 (JYFLTRAP, JYFL) ; [2] S. Eliseev *et al.*, PRC 83 (2011) 038501 (SHIPTRAP, GSI) ; [3] J. Suhonen, PRC 86 (2012) 024301 ; [4] M. Goncharov *et al.*, PRC 84 (2011) 028501 (SHIPTRAP, GSI) ; [5] J. Suhonen, PLB 701 (2011) 490 ; [6] S. Rahaman *et al.*, PRL 103 (2009) 042501 (JYFLTRAP, JYFL) ; [7] J. Suhonen, JPG 40 (2013) 075102 ; [8] D. A. Nesterenko *et al.*, PRC 86 (2012) 044313 (SHIPTRAP, GSI) ; [9] V. Kolhinen *et al.*, PLB 697 (2011) 116 (JYFLTRAP, JYFL)

Concise List of Other Cases ($\langle m_\nu \rangle = 0.3\,\text{eV}$) Part II

Transition	J_f^π	$Q-E$ [keV]	At. orb.	$T_{1/2}$ [yr]	Ref.
$^{144}\text{Sm} \rightarrow {}^{144}\text{Nd}$	2^+	171.89(87)	KL_3		[1]
$^{152}\text{Gd} \rightarrow {}^{152}\text{Sm}$	0^+_{gs}	0.91(18)	KL_1	$(1.1 - 1.7) \times 10^{28}$	[2] and [3]
$^{156}\text{Dy} \rightarrow {}^{156}\text{Gd}$	1^-	0.75(10)	KL_1		[4]
	0^+	0.54(24)	L_1L_1		[4]
	2^+	0.04(10)	M_1N_3		[4]
$^{162}\text{Er} \rightarrow {}^{162}\text{Dy}$	2^+	2.69(30) keV	KL_3		[5]
$^{164}\text{Er} \rightarrow {}^{164}\text{Dy}$	0^+_{gs}	6.81(13)	L_1L_1	$(3.6 - 5.8) \times 10^{32}$	[3] and [6]
$^{168}\text{Yb} \rightarrow {}^{168}\text{Er}$	(2^-)	1.52(25) keV	M_1M_3		[5]
$^{180}\text{W} \rightarrow {}^{180}\text{Hf}$	0^+_{gs}	11.24(27)	KK	$(4.4 - 11) \times 10^{30}$	[3] and [7]

[1] M. Goncharov *et al.*, PRC 84 (2011) 028501 (SHIPTRAP, GSI) ; [2] S. Eliseev *et al.*, PRL 106 (2011) 052504 (SHIPTRAP, GSI) ; [3] T.R. Rodríguez *et al.*, PRC 85 (2012) 044310 ; [4] S. Eliseev *et al.*, PRC 84 (2011) 012501(R) (SHIPTRAP, GSI) ; [5] S. Eliseev *et al.*, PRC 83 (2011) 038501 (SHIPTRAP, GSI) ; [6] S. Eliseev *et al.*, PRL 107 (2011) 052501 (SHIPTRAP, GSI) ; [7] A. Droese *et al.*, NPA 775 (2012) 1 (SHIPTRAP, GSI)

See the recent review: K. Blaum, S. Eliseev, F. A. Danevich, V. I. Tretyak, S. Kovalenko, M. I. Krivoruchenko, Yu. N. Novikov and J. S., Rev. Mod. Phys. 92 (2020) 045007.

The grand problem of $g_{\mathrm{A}}^{\mathrm{eff}}$

Motivation for the studies of $g_{\rm A}^{\rm eff}$

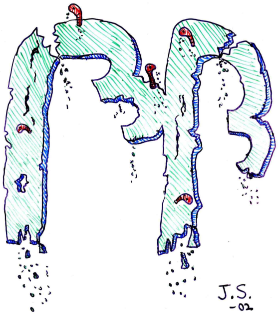

- DECAY:

$$2\nu\beta\beta - \text{rate} \sim \left| M^{(2\nu)}_{\rm GTGT} \right|^2 = (g_{\rm A})^4 \left| \sum_{m,n} \frac{M_{\rm L}(1^+_m) M_{\rm R}(1^+_n)}{D_m} \right|^2$$

$$0\nu\beta\beta - \text{rate} \sim \left| M^{(0\nu)}_{\rm GTGT} \right|^2 = (g_{{\rm A},0\nu})^4 \left| \sum_{J^\pi} (0^+_f || \mathcal{O}^{(0\nu)}_{\rm GTGT}(J^\pi) || 0^+_i) \right|^2$$

Example: $0\nu\beta\beta$ NMEs of ^{76}Ge, effect on the half-life

- Jiao *et al.*: Phys. Rev. C 96 (2017) 054310 (GCM+ISM)
- Menendez *et al.*: Nucl. Phys. A 818 (2009) 139 (ISM)
- Senkov *et al.*: Phys. Rev. C 93 (2016) 044334 (ISM)
- Barea *et al.*: Phys. Rev. C 91 (2015) 034304 (IBM-2)
- Suhonen: Phys. Rev. C 96 (2017) 055501 (pnQRPA + g_{pp} + isospin restoration + data on $2\nu\beta\beta$)

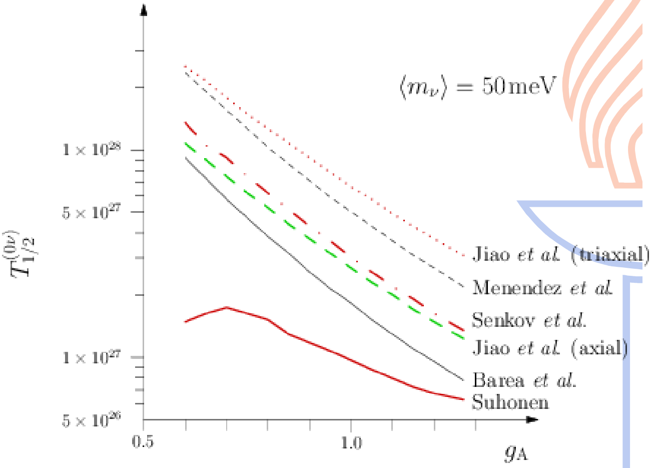

Let us open with the easiest part: Gamow-Teller β decays

There are data on:

Gamow-Teller β

TRANSITIONS

Theoretical approaches:

ISM (Interacting Shell Model)
pnQRPA (proton-neutron QRPA)

Typical Gamow-Teller β transitions

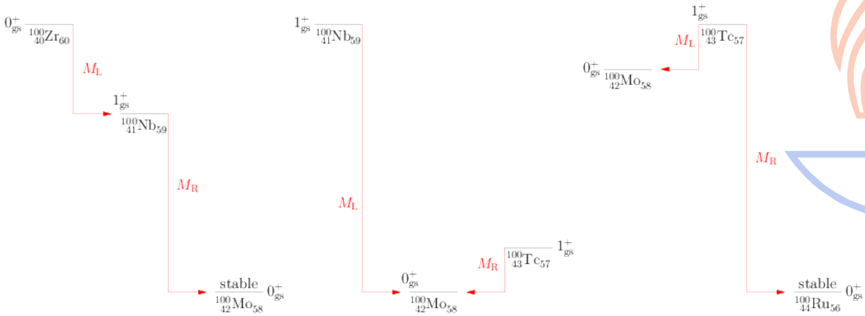

Results from:

Quenching of g_{A} in the ISM calculations

Results from the ISM

Mass range	g_A^{eff}	Reference
Full $0p$ shell	$1.03^{+0.03}_{-0.02}$	W. T. Chou *et al.* 1993
$0p$ – low$1s0d$ shell	$1.12^{+0.05}_{-0.04}$	D. H. Wilkinson *et al.* 1974
Full $1s0d$ shell	$0.96^{+0.03}_{-0.02}$	B. H. Wildenthal *et al.* 1983
	1.0	T. Siiskonen *et al.* 2001
$A = 41 - 50$ ($1p0f$ shell)	$0.937^{+0.019}_{-0.018}$	G. Martínez-Pinedo *et al.* 1996
$1p0f$ shell	0.98	T. Siiskonen *et al.* 2001
^{56}Ni	0.71	T. Siiskonen *et al.* 2001
$A = 52 - 67$ ($1p0f$ shell)	$0.838^{+0.021}_{-0.020}$	V. Kumar *et al.* 2016
$A = 67 - 80$ ($0f_{5/2}1p0g_{9/2}$ shell)	0.869 ± 0.019	V. Kumar *et al.* 2016
$A = 63 - 96$ ($1p0f0g1d2s$ shell)	0.8	M. Honma *et al.* 2006
$A = 76 - 82$ ($1p0f0g_{9/2}$ shell)	0.76	E. Caurier *et al.* 2012
$A = 90 - 97$ ($1p0f0g1d2s$ shell)	0.60	A. Juodagalvis *et al.* 2005
^{100}Sn	0.52	T. Siiskonen *et al.* 2001
$A = 128 - 130$ ($0g_{7/2}1d2s0h_{11/2}$ shell)	0.72	E. Caurier *et al.* 2012
$A = 130 - 136$ ($0g_{7/2}1d2s0h_{11/2}$ shell)	0.94	M. Horoi *et al.* 2016
$A = 136$ ($0g_{7/2}1d2s0h_{11/2}$ shell)	0.57	E. Caurier *et al.* 2012

Results from the ISM (illustration)

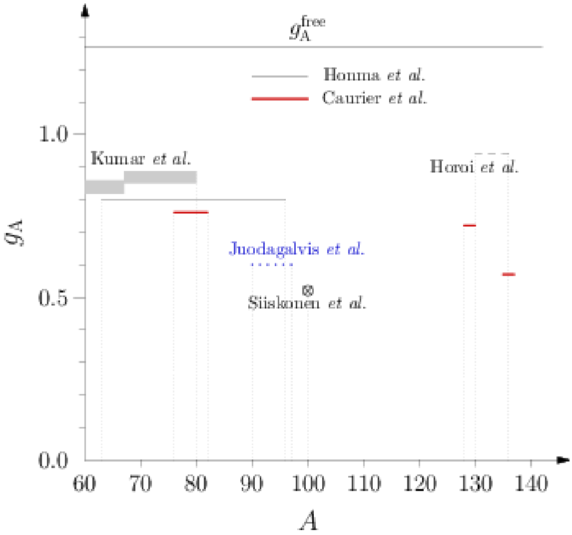

- Kumar *et al.*: J. Phys. G 43 (2016) 105104
- Honma *et al.*: J. Phys. Conf. Ser. 49 (2006) 45
- Caurier *et al.*: Phys. Lett. B 711 (2012) 62
- Horoi *et al.*: Phys. Rev. C 93 (2016) 024308
- Juodagalvis *et al.*: Phys. Rev. C 72 (2005) 024306
- Siiskonen *et al.*: Phys. Rev. C 63 (2001) 055501

Proton-neutron Quasiparticle Random-Phase Approximation (pnQRPA)

Results from:

Quenching of g_{A}

in the pnQRPA calculations

Results from the pnQRPA analyses

A	pn Conf.	$\bar{g}_A^{\rm eff}$ [1]
$62-70$	$1p_{3/2}-1p_{1/2}$	0.81 ± 0.20
$78-82$	$0g_{9/2}-0g_{9/2}$	0.88 ± 0.12
$98-116$	$0g_{9/2}-0g_{7/2}$	0.53 ± 0.13
$118-136$	$1d_{5/2}-1d_{5/2}$	0.65 ± 0.17
$138-142$	$1d_{5/2}-1d_{3/2}$	1.14 ± 0.10

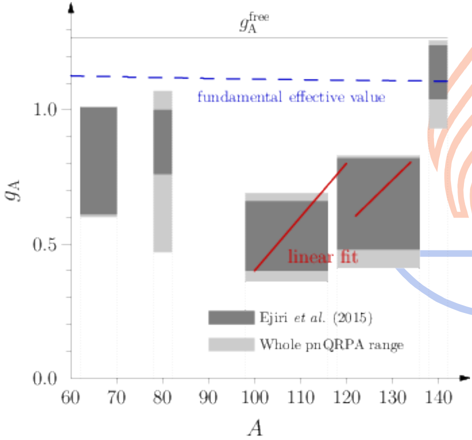

[1] H. Ejiri, J. S., J. Phys. G 42 (2015) 055201

Other analyses in the whole range:

[2] P. Pirinen, J. S., Phys. Rev. C 91 (2015) 054309

[3] F. Deppisch, J. S., Phys. Rev. C 94 (2016) 055501

Fundamental quenching: M. Ericson (1971); M. Ericson *et al.* (1973); M. Rho (1974); D. H. Wilkinson (1974)

(Meson-exchange currents → effective two-body operators)

Results from the ISM on top of the pnQRPA ranges

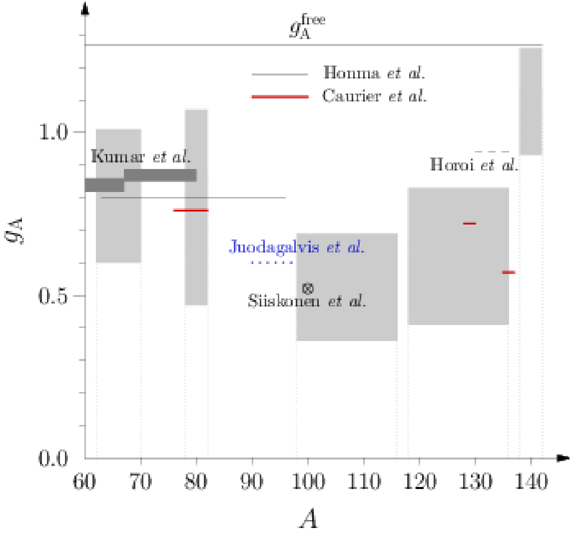

- Kumar *et al.*: J. Phys. G 43 (2016) 105104
- Honma *et al.*: J. Phys. Conf. Ser. 49 (2006) 45
- Caurier *et al.*: Phys. Lett. B 711 (2012) 62
- Horoi *et al.*: Phys. Rev. C 93 (2016) 024308
- Juodagalvis *et al.*: Phys. Rev. C 72 (2005) 024306
- Siiskonen *et al.*: Phys. Rev. C 63 (2001) 055501

Results from:

Quenching of g_A in the pnQRPA-based, ISM-based and IBM-based calculations of β decays and $\beta\beta$ decays

Interacting Boson Model (IBM) and its extensions

Collective fermion space

S ($J = 0$) and D ($J = 2$) collective fermion pairs (sub-space of the full ISM space, Pauli principle rules!)

$\Downarrow$ OAI mapping

IBM

s ($J = 0$) and d ($J = 2$) bosons (no Pauli principle) $H_{\rm F} \longrightarrow H_{\rm B}(s^\dagger, s, d^\dagger, d)$ (Otsuka-Arima-Iachello mapping)

proton and neutron $\Downarrow$ degrees of freedom

IBM-2

Microscopic IBM: Proton and neutron s and d bosons: $H_{\rm F} \longrightarrow H_{\rm IBM-2}$

Add one proton $\Downarrow$ or neutron fermion

IBFM-2

microscopic Interacting Boson-Fermion Model for odd-mass nuclei: $H_{\rm F} \longrightarrow H_{\rm IBFM-2}$

Add one proton$\Downarrow$ and neutron fermion

IBFFM-2

microscopic Interacting Boson-Fermion-Fermion Model for odd-odd mass nuclei: $H_{\rm F} \longrightarrow H_{\rm IBFFM-2}$

Results from the pnQRPA, IBM-2, and IBFFM-2

A	pnQRPA			IBFFM-2 [1]		IBM-2 [2]
	$g_A(\beta+\beta\beta)$ [3]	$g_A(\beta)$ [4]	$g_A(\beta\beta)$ [4]	$g_A(\beta)$	$g_A(\beta\beta)$	$g_A(\beta\beta)$
100	0.70 – 0.79	0.61 – 0.70	0.75 – 0.85	-	-	0.46(1) [SSD]
116	0.81 – 0.88	0.66 – 0.81	0.59 – 0.65	-	-	0.41(1) [SSD]
128	0.37 – 0.41	0.330 – 0.335	0.38 – 0.43	0.25 – 0.31	0.293	0.55(3) [CA]

[1] N. Yoshida, F. Iachello, Prog. Theor. Exp. Phys. 2013 (2013) 043D01 ; [2] J. Barea, J. Kotila, F. Iachello, Phys. Rev. C 87 (2013) 014315 ; [3] A. Faessler *et al.*, arXiv 0711.3996v1 [Nucl-th] ; [4] J. Suhonen, O. Civitarese, Nucl. Phys. A 924 (2014) 1

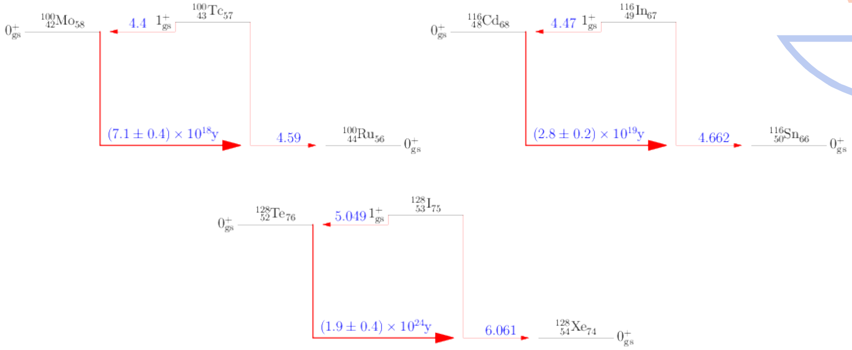

Results from the β+$\beta\beta$ calculations against the pnQRPA ranges from Gamow-Teller β decays

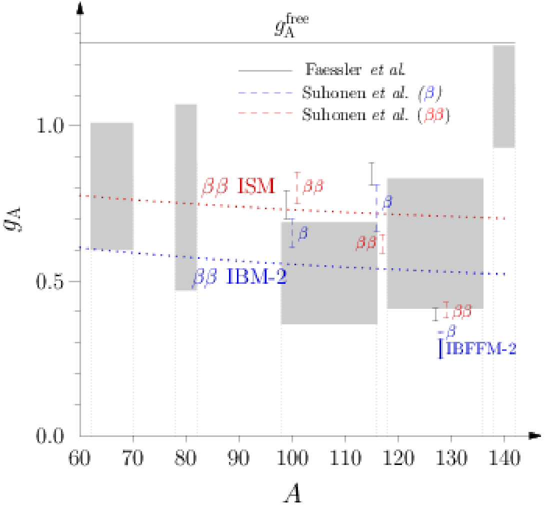

- Faessler *et al.*: A. Faessler, G. L. Fogli, E. Lisi, V. Rodin, A. M. Rotunno, F. Šimkovic, arXiv 0711.3996v1 [Nucl-th]
- Suhonen *et al.*: J. Suhonen, O. Civitarese, Nucl. Phys. A 924 (2014) 1
- $\beta\beta$ ISM and IBM-2: J. Barea, J. Kotila, F. Iachello, Phys. Rev. C 87 (2013) 014315

Collection of results extracted from the GT $\beta^{\pm}$/EC and $2\nu\beta\beta$ calculations

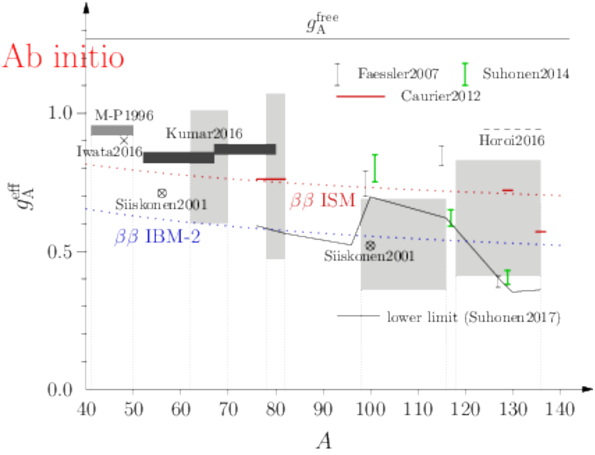

Ab initio: P. Gysbers *et al.*, Nature Physics 15 (2019) 428

- Faessler2007: pnQRPA A. Faessler *et al.*, arXiv 0711.3996v1 [Nucl-th]
- Suhonen2014: pnQRPA J. Suhonen *et al.*, Nucl. Phys. A 924 (2014) 1
- Suhonen2017: pnQRPA J. Suhonen, Phys. Rev. C 96 (2017) 055501
- Caurier2012: ISM E. Caurier *et al.*, Phys. Lett. B 711 (2012) 62
- Horoi2016: ISM M. Horoi *et al.*, Phys. Rev. C 93 (2016) 024308
- M-P1996: ISM G. Martínez-Pinedo *et al.*, Phys. Rev. C 53 (1996) R2602
- Iwata2016: ISM Y. Iwata *et al.*, Phys. Rev. Lett. 116 (2016) 112502
- Kumar2016: ISM V. Kumar *et al.*, J. Phys. G 43 (2016) 105104 Phys. Lett. B 711 (2012) 62
- Siiskonen2001: ISM T. Siiskonen *et al.*, Phys. Rev. C 63 (2001) 055501
- $\beta\beta$ ISM and IBM-2: J. Barea *et al.*, Phys. Rev. C 87 (2013) 014315
- Light hatched regions: pnQRPA H. Ejiri *et al.*, J. Phys. G 42 (2015) 055201 ; P. Pirinen *et al.*, Phys. Rev. C 91 (2015) 054309 ; F. Deppisch *et al.*, Phys. Rev. C 94 (2016) 055501

Spin-multipole NMEs

Results from:

Quenching of g_A as derived from spin-multipole NMEs of forbidden unique β decays

Spin-multipole (SM) nuclear matrix elements

General half-life formula for the allowed and unique-forbidden beta decays

$$t^K_{1/2}(0^+_{\rm gs} \leftrightarrow J^\pi) = \frac{\rm Constant}{\frac{g_{\rm A}{}^2}{2J_i+1}(M^K({\rm SM}J^\pi))^2 f_K} \ ,$$

where

- f_K is the phase-space factor for the K^{th} forbidden (allowed $\equiv 0^{th}$ forbidden) unique β-decay transition,
- $g_{\rm A}$ is the axial-vector coupling constant,
- $J_i = J$ or $J_i = 0$ ($J = K + 1$) is the angular momentum of the decaying state, and
- $M^K({\rm SM}J^\pi)$ is the spin-multipole NME for the K^{th} forbidden unique transition.

The unique decays are classified as:

K	0 (allowed)	1	2	3	4	5	6	7
J^π	1^+	2^-	3^+	4^-	5^+	6^-	7^+	8^-

Global study for the first-forbidden ($K = 1$) spin-dipole $2^-_{gs} \to 0^+_{gs}$ decays

H. Ejiri, N. Soukouti and J. S., Spin-dipole nuclear matrix elements for double beta decays and astro-neutrinos, Phys. Lett. B 729 (2014) 27

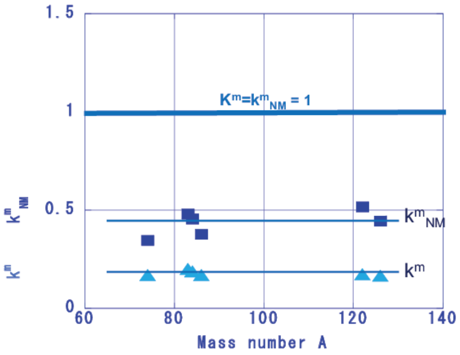

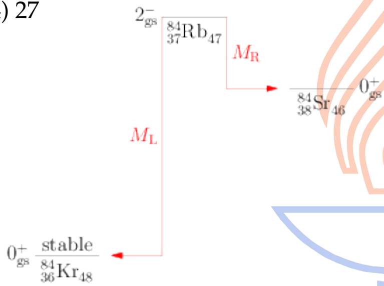

$$\bar{M}(SD2^-) = \sqrt{M_L M_R}$$

$$\langle k \rangle = \left\langle \frac{\bar{M}_{exp}(SD2^-)}{\bar{M}_{qp}(SD2^-)} \right\rangle \approx 0.18$$

$$\langle k_{NM} \rangle = \left\langle \frac{\bar{M}_{exp}(SD2^-)}{\bar{M}_{pnQRPA}(SD2^-)} \right\rangle \approx 0.45$$

$$\Rightarrow \bar{g}_A^{eff} \approx 0.57$$

Decays through higher spin-multipole ($K \geq 2$) operators

Question:

WHAT CAN WE LEARN

FROM THE UNIQUE HIGHER-FORBIDDEN

β DECAYS?

Answer:

A LOT!

INCENTIVE: $0\nu\beta\beta$ decay through the higher spin-multipole states

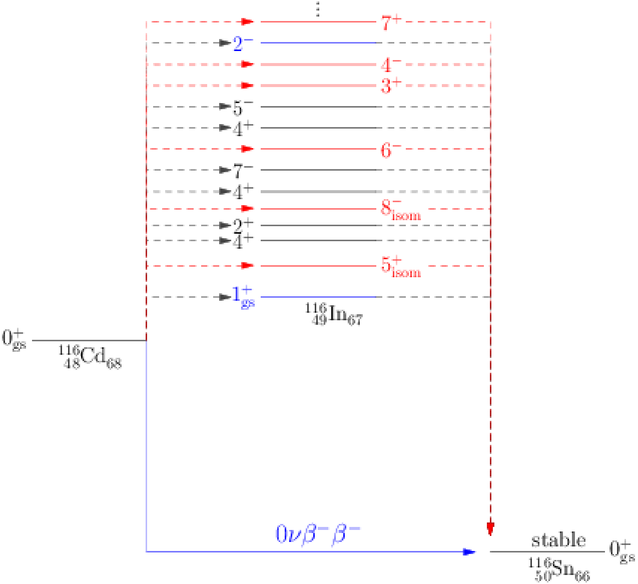

Decays through higher spin-multipole ($K \geq 2$) operators

Task:

STUDY 148 UNIQUE HIGHER-FORBIDDEN

β DECAYS IN ISOTOPIC CHAINS

Problem:

NO EXP. DATA AVAILABLE

Study:

$$k = \frac{M^K_{\rm pnQRPA}({\rm SM}J^\pi)}{M^K_{\rm qp}({\rm SM}J^\pi)} =?$$

Dependence on K and mass number A?

Example: Decays in the $A = 96$ chain

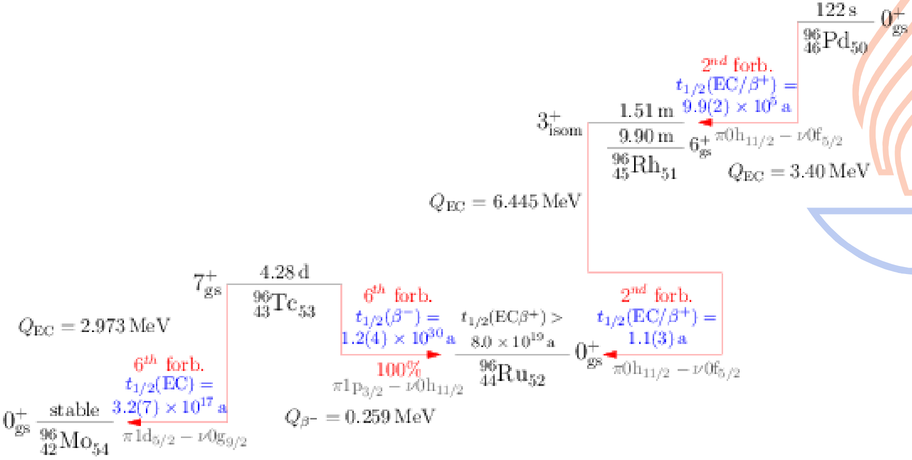

Example: Decays in the $A = 116$ chain

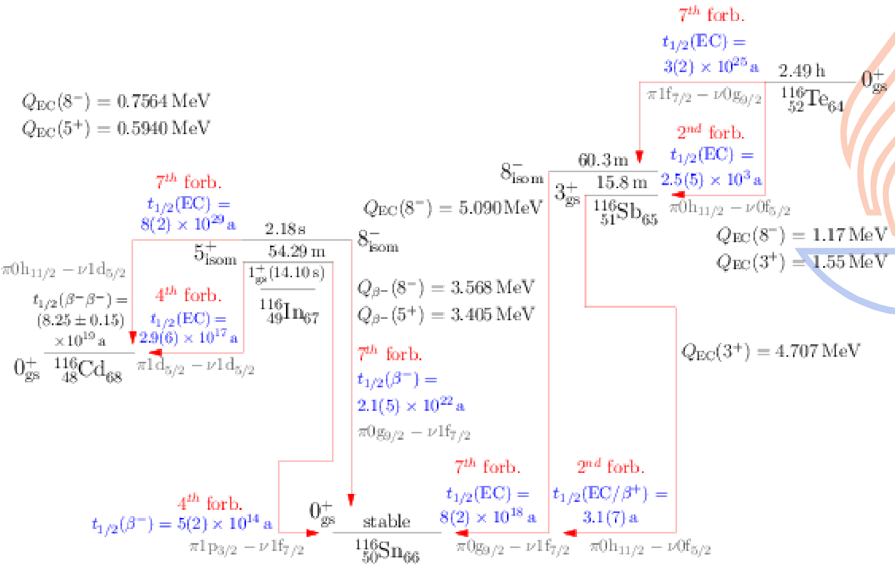

Example: Decays in the $A = 136$ chain

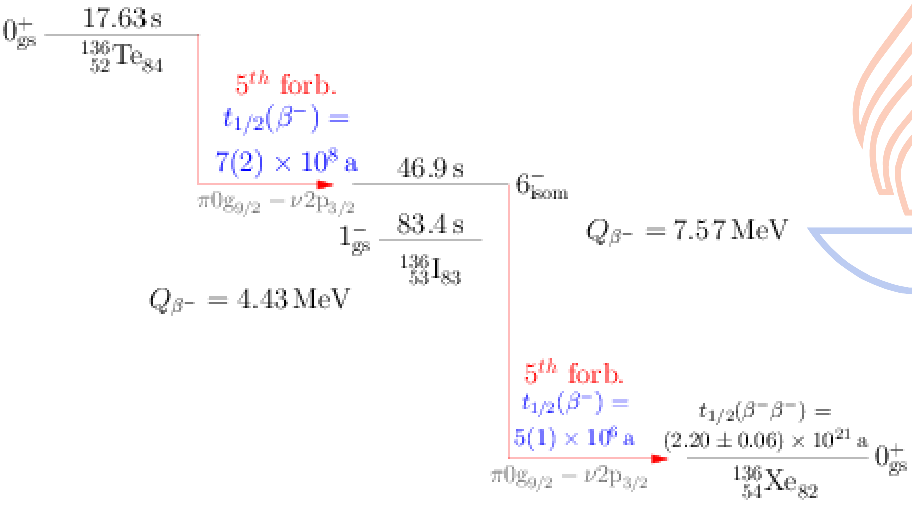

Example: Continuation of the $A = 136$ chain

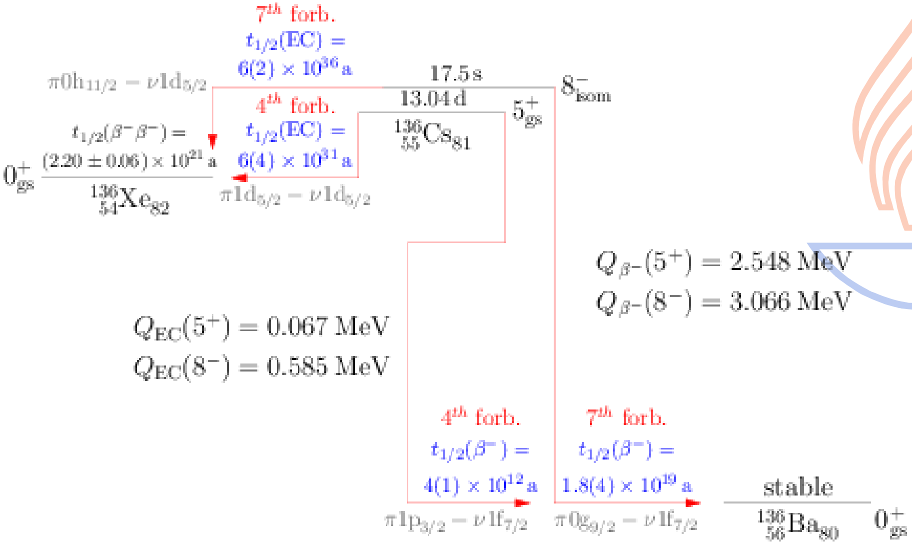

Ratio k for 74 β decays involving non-magic nuclei

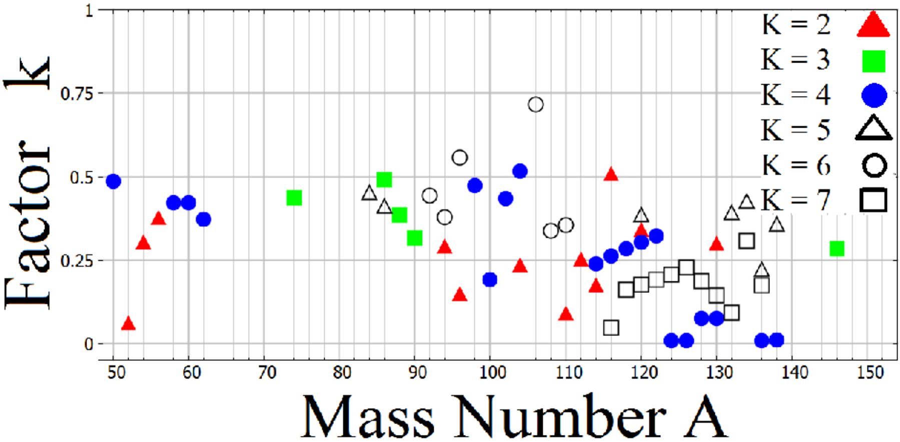

k extracted using the geometric mean of the full set of K^{th} ($K = 2 - 7$) forbidden β-decay transitions in an isobaric chain (J. Kostensalo, J. Suhonen, Phys. Rev. C 95 (2017) 014322)

Separation to β^- and β^+/EC decays

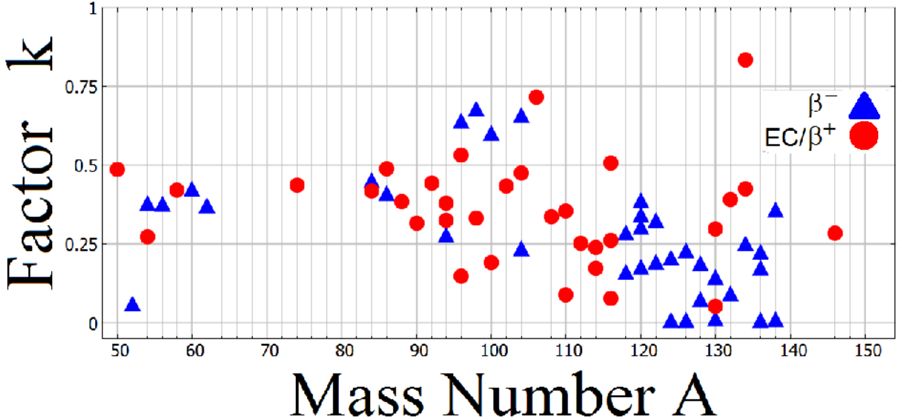

Results for the Ratio $k = M^K_{\rm pnQRPA}(SMJ^\pi)/M^K_{\rm qp}(SMJ^\pi)$

A	GT [1]	$K=1$ [2]	$K=2$	$K=3$	$K=4$	$K=5$	$K=6$	$K=7$	Avg.
$50-88$	0.35	0.40	0.25	0.46	0.43	0.43	-	-	0.39
$90-122$	0.52	0.40	0.25	0.35	0.34	0.38	0.41	0.13	0.31
$122-146$	0.40	0.40	0.30	0.28	0.07	0.35	-	0.19	0.24
Average	0.42	0.40	0.27	0.36	0.28	0.39	0.41	0.16	0.31

[1] H. Ejiri, J. S., J. Phys. G: Nucl. Part. Phys. 42 (2015) 055201

[2] H. Ejiri, N. Soukouti, J. S., Phys. Lett. B 729 (2014) 27

Conclusion: k is roughly independent of K $\Rightarrow$ Low-energy quenching of $g_{\rm A}$ derivable from the hatched regions of the Gamow-Teller studies in the pnQRPA framework:

Mass range	$A=76-82$	$A=100-116$	$A=122-136$
$g^{\rm eff}_{{\rm A},0\nu}$	$0.7-0.9$	0.5	$0.5-0.7$

Assumption: Also the forbidden non-unique virtual transitions behave like the forbidden unique virtual transitions.

Enhancement of the axial charge and quenching of g_A

Results from:

Effective value of g_A

as derived from

half-lives of

first-forbidden non-unique β decays

First-forbidden non-unique $J^+ \leftrightarrow J^-$ β decays

Enhancement of the time component of the axial current:

Nuclear matrix elements

$$g_A\mathcal{M}_{K+1,K,1} \text{ (unique transitions)} \; ; \; g_A\mathcal{M}_{K,K,1} \; ; \; g_V\mathcal{M}_{K,K,0} \; ; \; g_V\mathcal{M}_{K,K-1,1}$$

for K-fold forbidden β transitions emerge from the nucleonic current $j_N^\mu = g_V\gamma^\mu - g_A\gamma^\mu\gamma^5$.
Two additional contributions ($g_A\mathcal{M}_{0,1,1}$; $g_A\mathcal{M}_{0,0,0}$) for $J^+ \leftrightarrow J^-$ β decays:

$$\begin{array}{llcl} \text{space components} & g_A\gamma^k\gamma^5 & \longrightarrow & g_A\mathbf{r}\cdot\boldsymbol{\sigma} \\ \text{time component} & g_A\gamma^0\gamma^5 & \longrightarrow & g_A(\gamma^5)\frac{\boldsymbol{\sigma}\cdot\mathbf{p}_e}{M_Nc^2} \quad \text{(axial charge)} \end{array}$$

Axial-charge NME $g_A(\gamma^5)\mathcal{M}_{0,0,0}$

ENHANCED through $g_A(\gamma^5) = (1 + \varepsilon_{MEC})g_A$: Predicted 40 years ago by arguments based on soft-pion theorems and chiral symmetry. In the 90's studied from the perspective of exchange of heavy mesons.

Axial-charge strength as function of the mass number

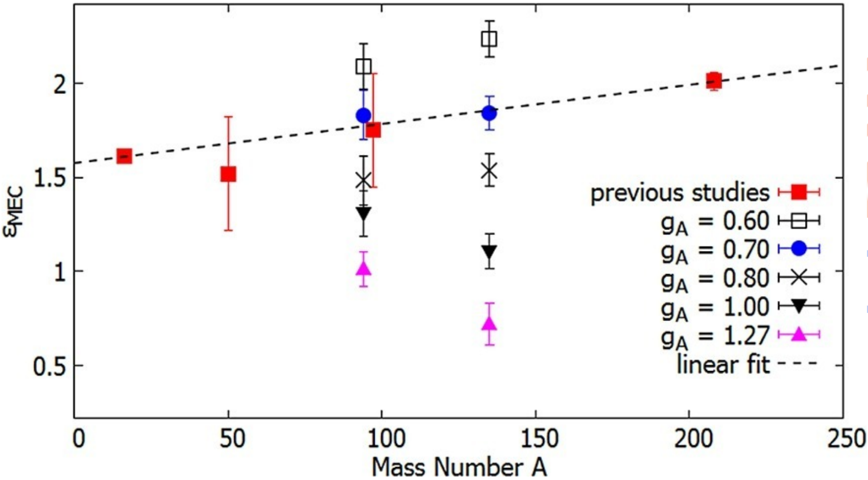

Previous studies: E. K. Warburton, I. S. Towner and B. A. Brown, Phys. Rev. C 49 (1994) 824 ; E. K. Warburton, J. A. Becker, B. A. Brown and D. J. Millener, Annals of Physics 187 (1988) 471 ; E. K. Warburton, Phys. Rev. C 44 (1991) 233.

Effect of axial-charge strength on β spectra

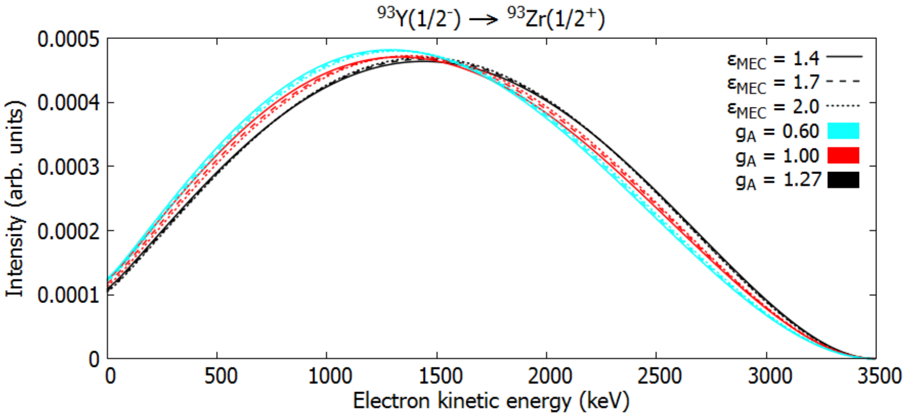

From: J. Kostensalo, J. S., Mesonic enhancement of the weak axial charge and its effect on the half-lives and spectral shapes of first-forbidden $J^+ \leftrightarrow J^-$ decays, Phys. Lett. B 781 (2018) 480 (computed by using the ISM).

Introducing the SSM: Spectrum-Shape Method

$$g_{A,0\nu}(J^\pi) \xrightarrow{q\to 0} g_A(J^\pi)$$

Higher-multipole transitions: Spectrum-Shape Method (SSM)*:

Effective value of $g_A(J^\pi)$

as derived from

electron spectra of

forbidden non-unique β decays

*First introduced in: M. Haaranen, P. C. Srivastava and J. S., Forbidden nonunique β decays and effective values of weak coupling constants, Phys. Rev. C 93 (2016) 034308

Half-life:

$$t_{1/2} = \kappa/\tilde{S}\,.$$

Dimensionless integrated shape function:

$$\tilde{S} = \int_1^{w_0} S(w_e)\mathrm{d}w_e\,, \quad S(w_e) = C(w_e) p w_\mathrm{e}(w_0 - w_e)^2 F_0(Z_f, w_e)\,.$$

Shape factor:

$$C(w_e) = \sum_{k_e,k_\nu,K} \lambda_{k_e} \left[M_K(k_e,k_\nu)^2 + m_K(k_e,k_\nu)^2 - \frac{2\gamma_{k_e}}{k_e w_e} M_K(k_e,k_\nu) m_K(k_e,k_\nu) \right],$$

where

$$\lambda_{k_e} = \frac{F_{k_e-1}(Z,w_e)}{F_0(Z,w_e)}\,; \quad \gamma_{k_e} = \sqrt{k_e^2 - (\alpha Z_f)^2}\,,$$

$F_{k-1}(Z,w_e)$ being the generalized Fermi function.

Decomposition of the shape factor:

$$C(w_e) = g_\mathrm{V}{}^2 C_\mathrm{V}(w_e) + g_\mathrm{A}{}^2 C_\mathrm{A}(w_e) + g_\mathrm{V} g_\mathrm{A} C_\mathrm{VA}(w_e).$$

EXAMPLE: 1*st*-forbidden nonunique decay of ^{140}Cs

First-forbidden nonunique β^- transition $^{140}\mathrm{Cs}(1^-) \rightarrow {}^{140}\mathrm{Ba}(0^+)$: a high-yield fission product$\longrightarrow$ Contributes to the reactor-flux anomalies!

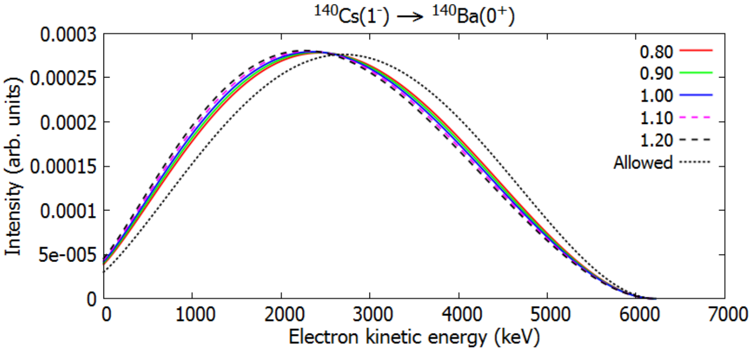

For the allowed approximation we have just a multiplicative factor and a universal spectral shape (independent of g_A): $C(w_e)_{\mathrm{allowed}} = \frac{1}{2J_i+1}\left(g_A{}^2 M_{\mathrm{GT}}^2 + g_V{}^2 M_{\mathrm{F}}^2\right) \neq$ function of w_e

ISM-computed β spectra for different values of g_A

Normalized ISM-computed electron spectra for the 2*nd*-forbidden nonunique β^- decays of ^{94}Nb and ^{98}Tc ($g_V = 1.0$).

From: J. Kostensalo and J. S., g_A-driven shapes of electron spectra of forbidden β decays in the nuclear shell model, Phys. Rev. C 96 (2017) 024317

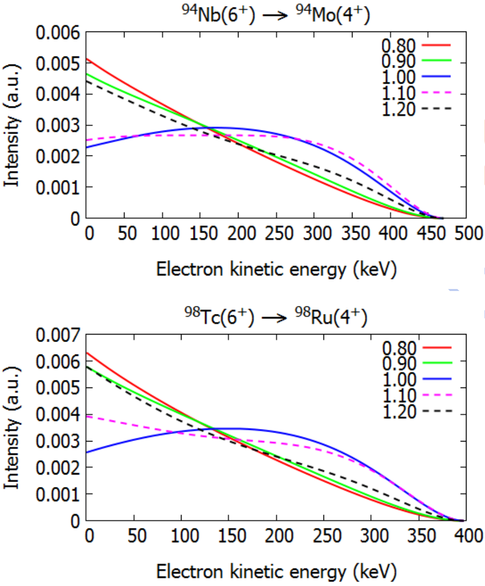

Example: ISM- and MQPM-computed electron spectra

Normalized electron spectra for the 2*nd*-forbidden nonunique β^- decay of ^{99}Tc ($g_V = 1.0$) using different values of g_A.

Going to be treated by the IBS-KNU-KRISS-LUKE-JYFL group: gA EXPERiment and Theory collaboration = gA-EXPERT and

the GSSI-INFN-LNGS-LUKE-JYFL Collaboration: Array of Cryogenic Calorimeters to Evaluate Spectral Shapes = ACCESS

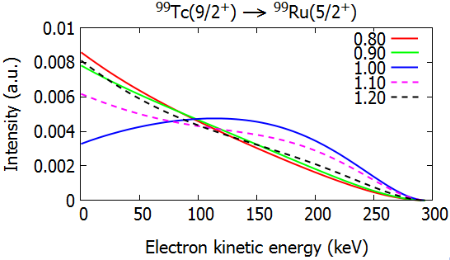

(ISM)

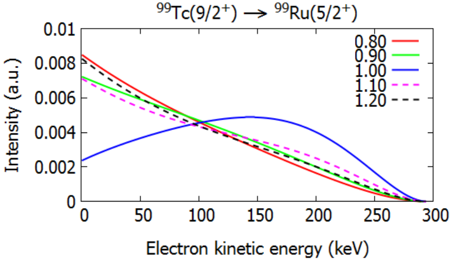

(MQPM)

Introducing the MQPM (Microscopic Quasiparticle-Phonon Model (MQPM) for odd-mass nuclei (J. Toivanen and J. S., Phys. Rev. C 57 (1998) 1237)

Single-particle space

particle creation: $c_a^\dagger$
($a =$ proton or $a =$ neutron)

$\Downarrow$ BCS

Quasiparticle mean field

quasiparticle creation: $a_a^\dagger$

QRPA $\Downarrow$ (for even-even nuclei)

Basic excitation:

$$\Gamma_{kJ}^\dagger = \sum_{a\leq b} \mathcal{N}_{ab}(J) \left(X_{ab}^k \left[a_a^\dagger a_b^\dagger\right]_J - Y_{ab}^k \left[a_a^\dagger a_b^\dagger\right]_J^\dagger \right)$$

$\Downarrow$ Bosonization leads to EOM

$$\begin{pmatrix} A & B \\ -B^* & -A^* \end{pmatrix} \begin{pmatrix} X^k \\ Y^k \end{pmatrix} = E_k \begin{pmatrix} X^k \\ Y^k \end{pmatrix}$$

$\Downarrow$ MQPM basic excitation

$$\Gamma_{lj}^\dagger = \sum_n C_n^l a_{nj}^\dagger + \sum_{a,kJ} D_{akJ}^l \left[a_a^\dagger \Gamma_{kJ}^\dagger\right]_j$$

$\Downarrow$ Equations of motion

$$\begin{pmatrix} A & B \\ B^{\mathrm{T}} & A' \end{pmatrix} \begin{pmatrix} C^l \\ D^l \end{pmatrix} = E_l \begin{pmatrix} 1 & 0 \\ 0 & N \end{pmatrix} \begin{pmatrix} C^l \\ D^l \end{pmatrix}$$

EXAMPLE: 1*st*-forbidden nonunique decay of ^{210}Bi

First-forbidden nonunique β^- transition $^{210}\mathrm{Bi}(1^-) \rightarrow {}^{210}\mathrm{Po}(0^+)$

Spectral shapes for different values of $g_{\mathrm{A}} = 0.80$(solid red), 0.90, 1.00, 1.10, 1.20(dashed black)

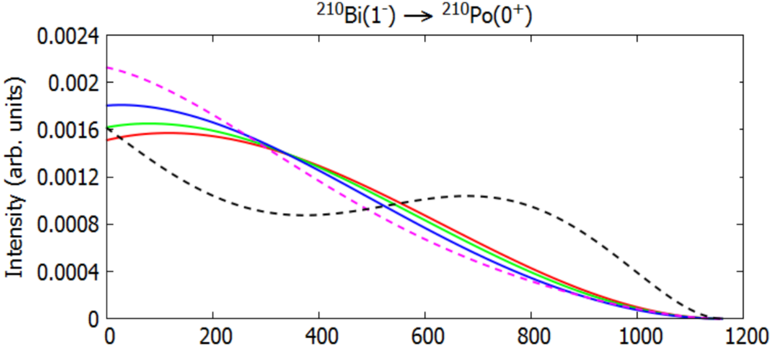

Measured and currently analyzed by the gA-EXPERT.

β spectral shapes without dependence on g_A

First-forbidden nonunique β^- decay

^{137}Xe$(7/2^-) \rightarrow {}^{137}Cs(7/2^+)$.

Normalized computed electron spectrum for the 2*nd*-forbidden nonunique β^- decay of ^{137}Cs

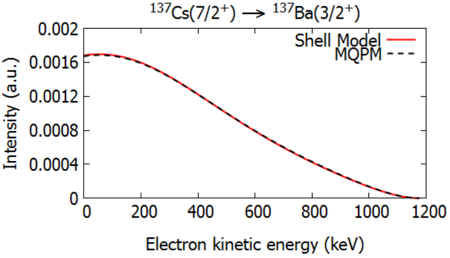

From: J. Kostensalo and J. S., Phys. Rev. C 96 (2017) 024317

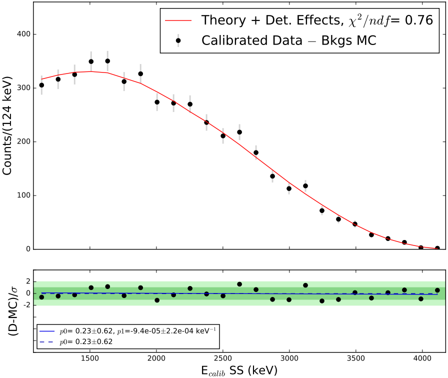

From: S. Al Kharusi *et al.* (EXO-200 Collaboration), Phys. Rev. Lett. 124 (2020) 232502.

Current list of g_A-dependent β-spectrum shapes

Transition	$J_i^{\pi_i}$ (gs)	$J_f^{\pi_f}$ (n_f)	Branching	K	Sensitivity	Nuclear model
^{59}Fe → ^{59}Co	$3/2^-$	$7/2^-$ (gs)	0.18%	2	Moderate	ISM
^{60}Fe → ^{60}Co	0^+	2^+ (gs)	**100%**	2	Moderate	ISM
^{87}Rb → ^{87}Sr	$3/2^-$	$9/2^+$ (gs)	**100%**	3	Moderate	MQPM, ISM
^{94}Nb → ^{94}Mo	6^+	4^+ (2)	**100%**	2	**Strong**	ISM
^{98}Tc → ^{98}Ru	6^+	4^+ (3)	**100%**	2	**Strong**	ISM
^{99}Tc → ^{99}Ru	$9/2^+$	$5/2^+$ (gs)	**100%**	2	**Strong**	MQPM, ISM
^{113}Cd → ^{113}In	$1/2^+$	$9/2^+$ (gs)	**100%**	4	**Strong**	MQPM, ISM, IBFM-2
^{115}In → ^{115}Sn	$9/2^+$	$1/2^+$ (gs)	**100%**	4	**Strong**	MQPM, ISM, IBFM-2
^{136}Te → ^{136}I	0^+	(1^-) (gs)	**8.7%**	1	**Strong**	ISM
^{137}Xe → ^{137}Cs	$7/2^-$	$5/2^+$ (1)	**30%**	1	**Strong**	ISM
^{138}Cs → ^{138}Ba	3^-	3^+ (1)	**44%**	1	**Strong**	ISM
^{210}Bi → ^{210}Po	1^-	0^+ (gs)	**100%**	1	**Strong**	ISM

- Electron spectra of ^{113}Cd (L. Bodenstein-Dresler *et al.*, Phys. Lett. B 800 (2020) 135092) measured by the COBRA collaboration.
- Electron spectrum of ^{115}In measured by using $LiInSe_2$ bolometers (Experimentalists-Jyväskylä collaboration).

EXAMPLE: 4*th*-forbidden nonunique decay of ^{113}Cd

4*th*-forbidden nonunique β^- transition $^{113}\mathrm{Cd}(1/2^+) \rightarrow {}^{113}\mathrm{In}(9/2^+)$

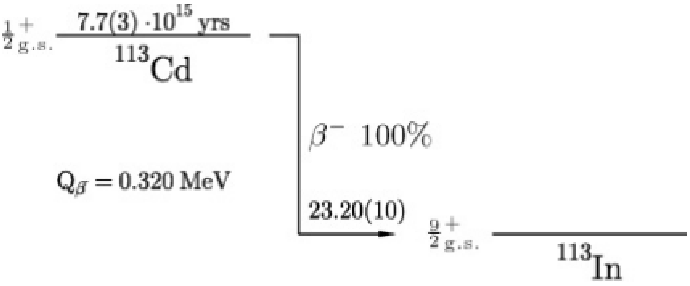

Calculated by using the Interacting Shell Model (ISM), the Microscopic Quasiparticle-Phonon Model (MQPM) and the microscopic Interacting Boson-Fermion Model (IBFM-2).

Decay of ^{113}Cd – Comparison with data

Normalized electron spectra for the 4*th*-forbidden nonunique β^- transition $^{113}\mathrm{Cd}(1/2^+) \rightarrow {}^{113}\mathrm{In}(9/2^+)$ ($g_\mathrm{V} = 1.0$).

Experimental data from The COBRA collaboration: PLB2020: L. Bodenstein-Dresler *et al.*, Phys. Lett. B 800 (2020) 135092.

Measured spectrum by detector no. 54:

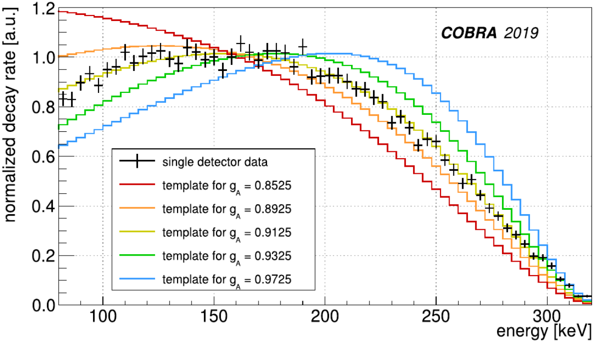

Decay of ^{113}Cd – Comparison with data

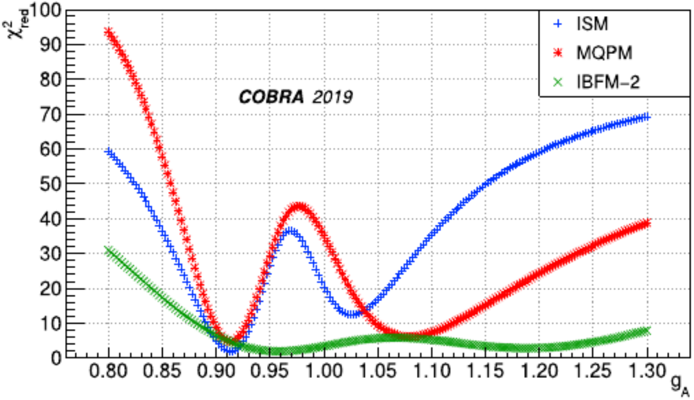

PLB2020 : $\bar{g}_A$(ISM) $= 0.914 \pm 0.008$; PLB2021 $:= 0.907 \pm 0.064$
PLB2020 : $\bar{g}_A$(MQPM) $= 0.910 \pm 0.013$; PLB2021 $:= 0.993 \pm 0.063$
PLB2020 : $\bar{g}_A$(IBFM-2) $= 0.955 \pm 0.035$; PLB2021 $:= 0.828 \pm 0.140$

Decay of ^{113}Cd – $g_A^{\rm eff}$ using spectral moments

SMM = Spectral Moments Method

$$\mu_n = \int_{w_{\rm thr}}^{w_0} S(w_e) w_e^n {\rm d}w_e \,,$$

$n = 0 \leftrightarrow$ area under the spectral curve $\leftrightarrow T_{1/2}$

$n = 1 \leftrightarrow$ mean energy

$n = 2 \leftrightarrow$ variance

Usually only first few moments μ are enough!

Result from

J. Kostensalo, E. Lisi, A. Marrone and J. S., ^{113}Cd β-decay spectrum and g_A quenching using spectral moments, Phys. Rev. C 107 (2023) 055502.

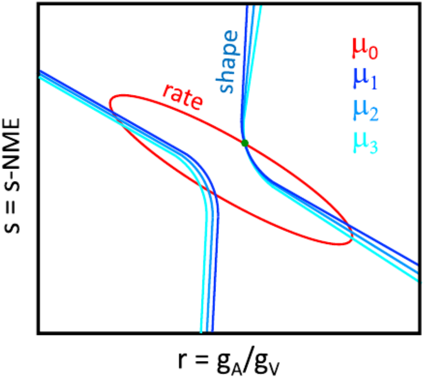

$$\bar{g}_{\rm A}({\rm ISM}) = 0.96 - 0.99$$
$$\bar{g}_{\rm A}(\text{IBFM-2}) = 1.03 - 1.13$$
$$\bar{g}_{\rm A}({\rm MQPM}) = 1.02 - 1.07$$

EXAMPLE: 4*th*-forbidden nonunique transition $^{115}\text{In}(9/2^+) \rightarrow {}^{115}\text{Sn}(1/2^+)$

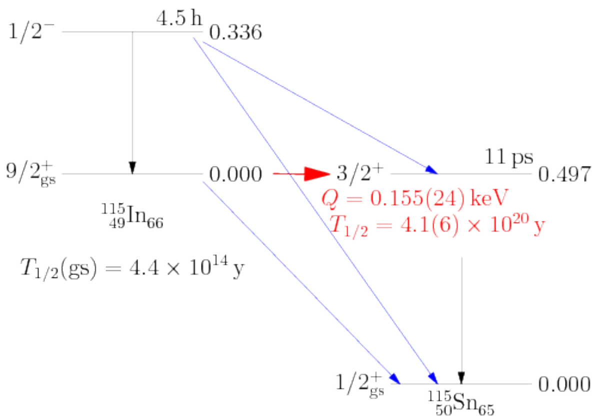

Interesting ultra-low Q-value transition: The 2*nd*-forbidden unique transition $^{115}\text{In}(9/2^+) \rightarrow {}^{115}\text{Sn}(3/2^+)$ has the smallest known Q value of a nuclear transition: J. S. E. Wieslander *et al.*, Phys. Rev. Lett. 103 (2009) 122501; B. J. Mount *et al.*, Phys. Rev. Lett. 103 (2009) 122502.

Decay of ^{115}In – Comparison with data

Normalized electron spectra for the 4*th*-forbidden nonunique β^- decay $^{115}\text{In}(9/2^+) \to {}^{115}\text{Sn}(1/2^+)$ ($g_V = 1.0$).

Result from

The CEA-CNRS-CSNSM-INR-JYFL-MIT-LUKE-UCB collaboration: A. F. Leder *et al.*, Phys. Rev. Lett. 129 (2022) 232502.

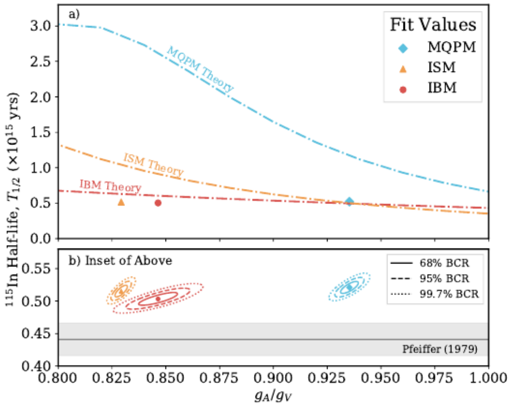

$$\bar{g}_A(\text{ISM}) = 0.830 \pm 0.002$$
$$\bar{g}_A(\text{IBFM-2}) = 0.845 \pm 0.006$$
$$\bar{g}_A(\text{MQPM}) = 0.936 \pm 0.003$$

Conclusions about the effective g_A

Conclusion 1:

The long chain of ISM calculations and the recent pnQRPA and IBM-2 calculations of Gamow-Teller β decays and $2\nu\beta\beta$ decays are (surprisingly!) consistent with each other and clearly point to a A-dependent quenched g_A

Conclusion 2:

The spectrum-shape method (SSM) and the spectral moments method (SMM) for forbidden non-unique β decays seem robust tools (largely independent of the nuclear model, the assumed Hamiltonian and mean field) to search for the effective value of g_A and to try to solve other problems, like those related to the reactor-$\bar{\nu}_e$ spectra

Spectral shapes as background: Total β spectrum of ^{214}Pb

^{85}Kr, ^{212}Pb and ^{214}Pb are backgrounds in dark-matter experiments like XENON1T, XENONnT, PandaX, etc. (see S. J. Haselschwardt et al., Phys. Rev. C 102 (2020) 065501.

Beta decay of ^{214}Pb includes several first-forbidden non-unique transitions from 0^+ to 0^- and 1^- states within the decay Q window.

Total spectrum from M. Ramalho *et al.*, in collaboration with the PandaX dark-matter experiment

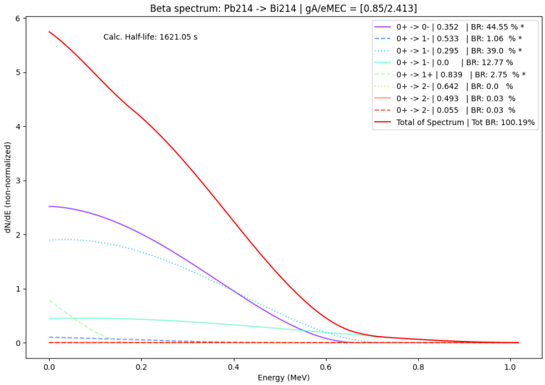

Still more spectral shapes: β spectra of fission yields

Investigating

Reactor-$\bar{\nu}$ anomaly

and

the spectral bump

Neutrino-related anomalies and sterile neutrinos

Sterile neutrinos:

The gallium anomaly

(J. Kostensalo, J. S., C. Giunti and P. C. Srivastava,

The gallium anomaly revisited, Phys. Lett. B 795 (2019) 542)

The reactor antineutrino anomaly

imply oscillations of the "ordinary" neutrinos (ν_e, ν_μ, ν_τ) to

STERILE NEUTRINO

in the mass range of a few eV

But what is the reactor antineutrino anomaly?

The reactor antineutrino anomaly

The $\bar{\nu}_e$ flux from reactors has been measured in short-baseline neutrino-oscillation experiments[1]: Daya Bay (in Daya Bay, China; 6 reactors, 8 detectors), RENO (South Korea; 2 detectors 294m and 1383 m from 6 reactors) and Double Chooz (Chooz, France, 2 detectors 400m and 1050 m from 2 reactors, schematic figure below).

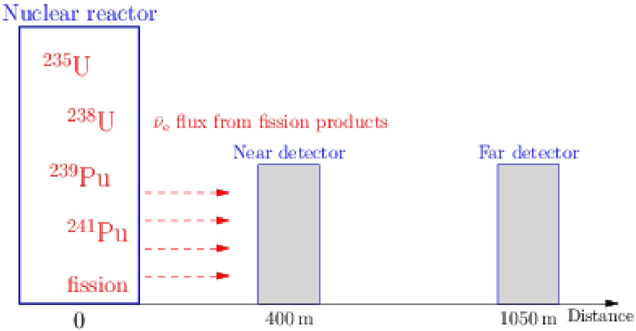

[1] RENO: Phys. Rev. Lett. 108 (2012) 191802; Double Chooz: J. High Energy Phys. 2014 (2014) 86; Daya Bay: Phys. Rev. Lett. 116 (2016) 061801.

The neutrino-flux measurements find:

The reactor $\bar{\nu}_e$ anomaly:

The measured flux is some 5% smaller than that predicted from the β decays of the fission yields of the reactor fuel

$\stackrel{?}{\Longrightarrow}$ Oscillations to STERILE NEUTRINOS

The bump anomaly:

There is an unexpected bump at $4-6$ MeV (spectral shoulder) in the measured $\bar{\nu}_e$ spectrum.

$\Longrightarrow$???

Important contributions from first-forbidden β decays to the reactor antineutrino spectra (deviations from the allowed spectral shape)

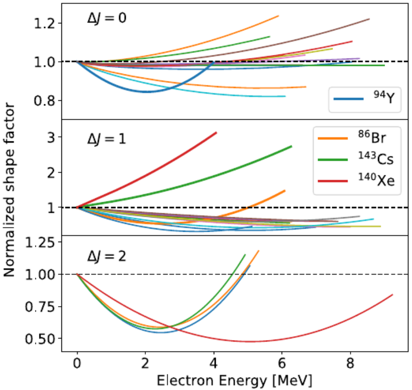

pseudoscalar ($\Delta J = 0$, non-unique),

pseudovector ($\Delta J = 1$, non-unique) and

pseudotensor ($\Delta J = 2$, unique) transitions

Pseudovector transitions with (^{136}Te) and without (^{140}Xe) g_A dependence

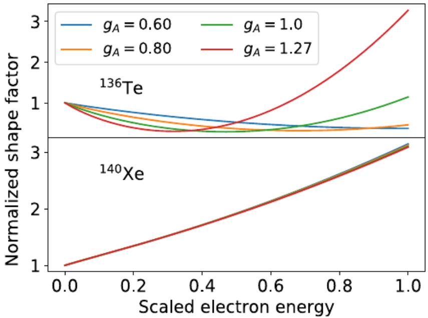

The transitions $^{137}\mathrm{Xe}(7/2^-) \to {}^{137}\mathrm{Cs}(7/2^+_{\mathrm{gs}}, 5/2^+_1)$ are highly interesting: Measurement of the spectral shapes by EXO-200

Results from the analyses including the β spectra

Taking into account the (first-forbidden) decays of ^{86}Br(0^+), ^{86}Br(2^+), ^{87}Se, ^{88}Rb, ^{89}Br($3/2^+$), ^{89}Br($5/2^+$), ^{90}Rb, ^{91}Kr($5/2^-$), ^{91}Kr($3/2^-$), ^{92}Rb, ^{92}Y, ^{93}Rb, ^{94}Y(0^+), ^{94}Y(0^+), ^{95}Rb($7/2^+$), ^{95}Rb($3/2^+$), ^{95}Sr, ^{96}Y, ^{97}Y, ^{98}Y, ^{133}Sn, ^{134m}Sb(6^+), ^{134m}Sb(6^+?), ^{135}Te, ^{136m}I, ^{137}I, ^{138}I, ^{139}Xe, ^{140}Cs, ^{142}Cs

changes the $\bar{\nu}$ flux by a few % !

HKSS flux model:

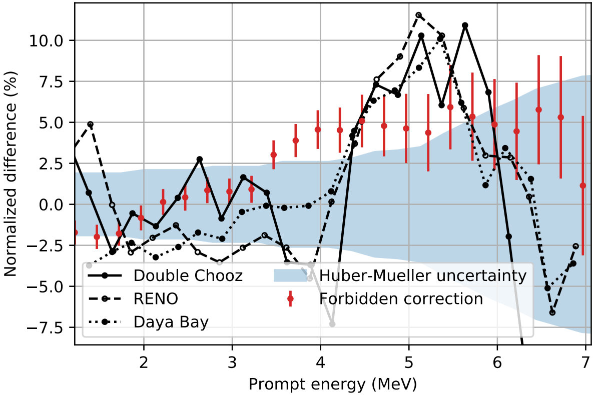

The spectral shoulder appears due to forbidden spectral corrections !

See: L. Hayen, J. Kostensalo, N. Severijns, J.S., First-forbidden transitions in reactor antineutrino spectra/in the reactor anomaly, Phys. Rev. C 99 (2019) 031301(R) ; Phys. Rev. C 100 (2019) 054323

Pioneering calculation of a total β-electron spectrum of a high-Q reactor fission product: The β^- decay of ^{92}Rb with a Q value of 8.095 MeV

Computed cumulative electron spectrum

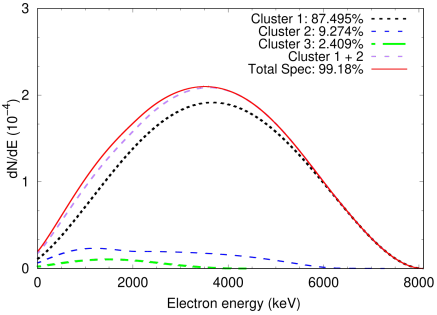

Cluster 1: gs-to-gs transition (based on TAS-measured branching), Cluster 2: known 1*st*-forbidden transitions (based on TAS-measured branchings), Cluster 3: unresolved higher-energy 1*st*-forbidden and allowed transitions

Comparison of the computed total spectrum with the TAS spectrum. Computations done by using two available shell-model interactions.

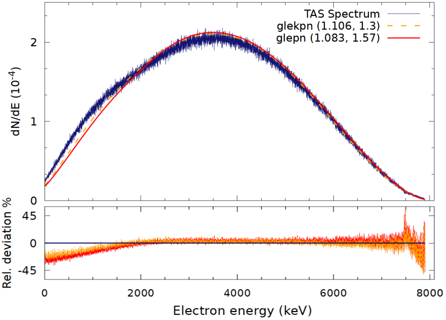

TAS spectrum obtained from the TAS-measured (A. Algora *et co.*) branchings assuming all transitions to be allowed.

Small sidestep to

the gallium anomaly

and

charge-exchange reactions

Charged-current neutrino-^{71}Ga scattering via Gamow-Teller type of transitions.

Monoenergetic ν_e from artificial neutrino sources via Electron captures:

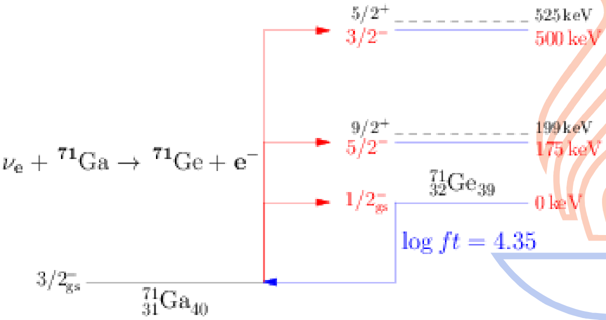

$$^{37}\text{Ar} + e^- \to {}^{37}\text{Cl} + \nu_e \ (E_\nu = 814\,\text{keV})\ ; \quad {}^{51}\text{Cr} + e^- \to {}^{51}\text{V} + \nu_e \ (E_\nu = 751\,\text{keV})$$

The scattering cross sections σ have been measured by the GALLEX experiment [Phys. Lett. B 342 (1995) 440 ; ibid B 420 (1998) 114 ; ibid B 685 (2010) 47] and the SAGE experiment [Phys. Rev. Lett. 77 (1996) 4708 ; Phys. Rev. C 59 (1999) 2246 ; ibid C 73 (2006) 045805 ; ibid C 80 (2009) 015807]

Estimation of the scattering cross section

The cross sections can be deduced from neutrino kinematics, as first done by J. N. Bahcall, Phys. Rev. C 56 (1997) 3391 (verified by our more complete calculations)

$$\sigma(^{37}\mathrm{Ar}) = 6.62 \times 10^{-45}\,\mathrm{cm}^2 \left(1 + 0.695\frac{\mathrm{BGT}_{175}}{\mathrm{BGT}_{\mathrm{gs}}} + 0.263\frac{\mathrm{BGT}_{500}}{\mathrm{BGT}_{\mathrm{gs}}}\right) .$$

$$\sigma(^{51}\mathrm{Cr}) = 5.53 \times 10^{-45}\,\mathrm{cm}^2 \left(1 + 0.667\frac{\mathrm{BGT}_{175}}{\mathrm{BGT}_{\mathrm{gs}}} + 0.218\frac{\mathrm{BGT}_{500}}{\mathrm{BGT}_{\mathrm{gs}}}\right) ,$$

where $\mathrm{BGT}_{\mathrm{gs}}$ can be normalized by the $\log ft$ of the Gamow-Teller EC transition $^{71}\mathrm{Ge}(1/2^-_{\mathrm{gs}}) \rightarrow ^{71}\mathrm{Ga}(3/2^-_{\mathrm{gs}})$, and $\mathrm{BGT} = (g_{\mathrm{A}})^2 (f||\mathcal{O}_{\mathrm{GT}}||i)^2/(2J_i+1)$, J_i being the angular momentum of the initial state.

BGT ratios can be taken from D. Frekers *et al.*, The $^{71}\mathrm{Ga}(^3\mathrm{He},t)$ reaction and the low-energy neutrino response, Phys. Lett B 706 (2011) 134:

$$\frac{\mathrm{BGT}_{175}}{\mathrm{BGT}_{\mathrm{gs}}} = 0.039 \pm 0.030\,; \quad \frac{\mathrm{BGT}_{500}}{\mathrm{BGT}_{\mathrm{gs}}} = 0.202 \pm 0.016\,,$$

or from our shell-model calculations with the JUN45 interaction:

$$\frac{\mathrm{BGT}_{175}}{\mathrm{BGT}_{\mathrm{gs}}} = 0.033\,; \quad \frac{\mathrm{BGT}_{500}}{\mathrm{BGT}_{\mathrm{gs}}} = 0.016\,,$$

Quantitative statement of the gallium anomaly

$$R = \frac{\sigma_{\text{measured}}(\text{GALLEX,SAGE})}{\sigma_{\text{estimated}}}.$$

It seems that experiments measure a reduced neutrino flux:

Estimate	GALLEX 1	GALLEX 2	SAGE 1	SAGE 2
R(Frekers *et al.*)	0.93 ± 0.11	0.79 ± 0.11	0.93 ± 0.11	0.77 ± 0.08
R(SM, JUN45)	0.98 ± 0.11	0.83 ± 0.11	0.97 ± 0.12	0.81 ± 0.09

$\overset{?}{\Longrightarrow}$ Oscillations to STERILE NEUTRINOS

Questions raised:

- Are there problems with the cross-section measurements (GALLEX 1 vs. GALLEX 2, SAGE 2)?
- Why the BGT of Frekers *et al.* deviate from our shell-model computed BGTs?

$$\mathrm{BGT}_{\mathrm{reaction}} = \frac{(g_{\mathrm{A}})^2}{2J_i+1}\left[(f\|\mathcal{O}_{\mathrm{GT}}\|i) + \delta(f\|\mathcal{O}_{\mathrm{T}}\|i)\right]^2,$$

where $\mathcal{O}_{\mathrm{T}} \sim [\sigma Y_2]_1$ is the tensor part entering the reaction analysis and $\delta = 0.097$ is the mixing strength (From the analysis of Gamow-Teller transitions in the sd shell: W.C. Haxton, Phys. Lett. B 431 (1998) 110.).

We find interference of the GT and tensor terms:

Transition	$(f\|\mathcal{O}_{\mathrm{GT}}\|i)$	$(f\|\mathcal{O}_{\mathrm{T}}\|i)$	BGT_{β}(SM)	$\mathrm{BGT}_{\mathrm{reaction}}$(SM)
$3/2^-$(Ga) $\to$ $1/2^-$(Ge, gs)	-0.795	0.465	0.158	0.141
$3/2^-$(Ga) $\to$ $5/2^-$(Ge, 175 keV)	0.144	-1.902	0.0052	0.0004
$3/2^-$(Ga) $\to$ $3/2^-$(Ge, 500 keV)	0.100	0.048	0.0025	0.0027

The charge-exchange reactions assume always a constructive interference of the GT and tensor terms!

Conclusions about the ^{71}Ga anomaly

Conclusions:

NONE YET!

The work continues. . .

Low Q values: spectral shapes and Breit-Wigner resonances

Low Q-value β^-/EC decays for (anti)neutrino-mass measurements

$$\boxed{\beta^- : (A, Z) \rightarrow (A, Z+1) + e^- + \bar{\nu}_e}$$

$$\boxed{\mathrm{EC} : (A, Z) + e^- \rightarrow (A, Z-1) + \nu_e}$$

Neutrino Mass Measurements with low Q values

The KArlsruhe TRItium Neutrino experiment = KATRIN

$Q_{\beta^-} = 18.6\,\text{keV}$, Allowed
$^{3}\text{H}(1/2^+) \to {}^{3}\text{He}(1/2^+)$ β^- decay, $T_{1/2} = 12.33\,\text{y}$
Sensitivity to neutrino mass: $m_\nu \sim 0.2\,\text{eV}$

$\Downarrow$

(The Microcalorimetric Array for a Rhenium Experiment = MARE

$Q_{\beta^-} = 2.469(4)\,\text{keV}$, First-forbidden unique $^{187}\text{Re}(5/2^+) \to {}^{187}\text{Os}(1/2^-)$ β^- decay, $T_{1/2} = 4 \times 10^{10}$ y)

The Electron Capture in Holmium experiment = ECHo
$Q_{\text{EC}} = 2.833(34)\,\text{keV}$ (Penning trap), Allowed $^{163}\text{Ho}(7/2^-) \to {}^{163}\text{Dy}(5/2^-)$ EC decay,
$T_{1/2} = 4570\,\text{y}$
Sensitivity to neutrino mass: $m_\nu \sim ?$

$\Downarrow$

?

Extraction of the neutrino mass

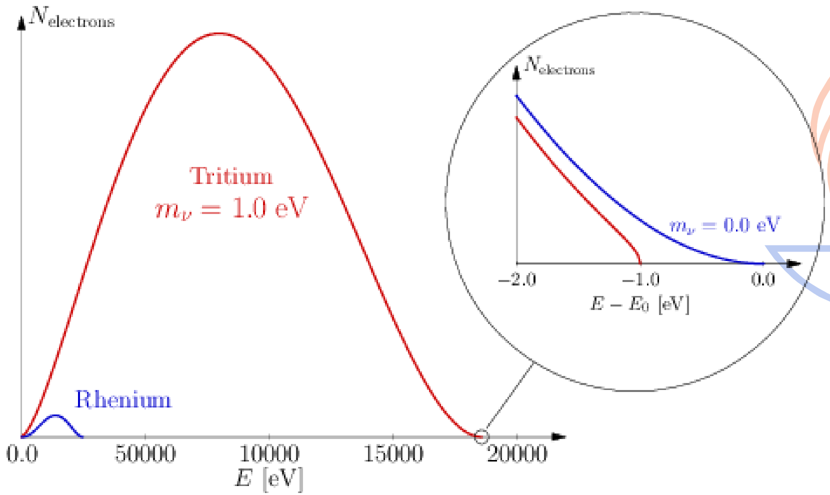

The fraction of decays in an energy interval ΔE near the endpoint goes as $(\Delta E/Q)^3$

Decays (1st and 2nd forbidden unique) of ^{135}Cs to excited states

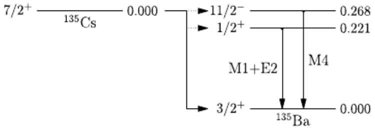

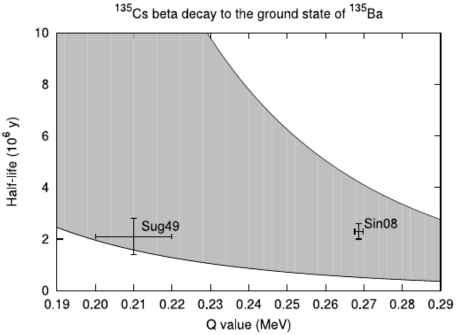

M.T. Mustonen and J. S., PLB 703 (2011) 370:

Important to revisit the Q-value msrmt!

Recent measurement of the Q value by the JYFLTRAP gives $Q = 268.66(30)$ keV, leading to $Q_{\rm exc} = 0.44(31)$ keV for the first-forbidden unique transition ^{135}Cs$(7/2^+) \rightarrow$ ^{135}Ba$(11/2^-)$.

Adopting $g_A^{\rm eff} = 0.8 - 1.2$ leads to half-life prediction:

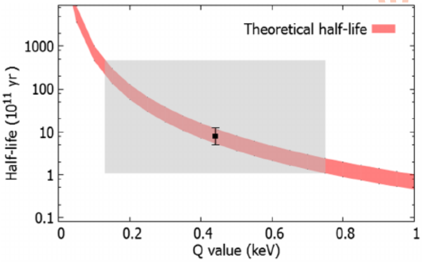

A. de Roubin *et al.*, Phys. Rev. Lett. 124 (2020) 222503 gs-gs Q value improved over the AME2020 mass evaluation:

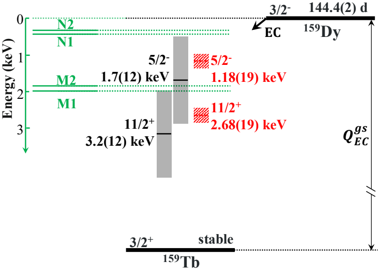

Recent measurement of the Q value by the JYFLTRAP gives $Q = 364.73(19)$ keV, leading to $Q_{\rm exc} = 1.18(19)$ keV for the allowed β transition ^{159}Dy$(3/2^-) \to$ ^{159}Tb$(5/2^-)$.

One has the N1, N2, O1, O2 and P1 (and M1 and M2 Breit-Wigner tails!) atomic-shell contributions at the endpoint:

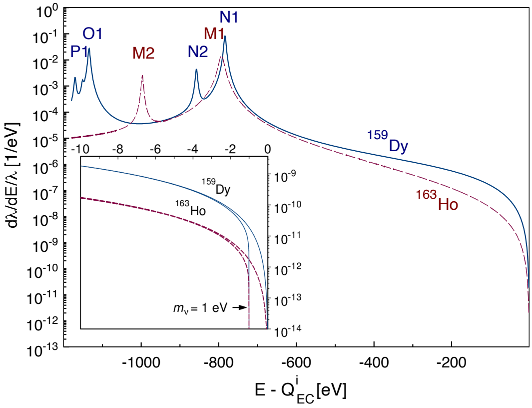

A new candidate for neutrino-mass determination!

Z. Ge *et al.*, Phys. Rev. Lett. 127 (2021) 272301

Allowed electron-capture decay of ^{111}In to an excited state

gs-gs Q value improved over the AME2020 mass evaluation:

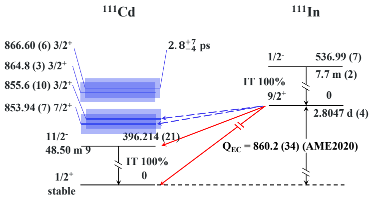

A new candidate for neutrino-mass determination!

Z. Ge *et al.*, Phys. Lett. B 832 (2022) 137226

Recent measurement of the Q value by the JYFLTRAP gives $Q = 857.63(17)$ keV, leading to $Q_{\rm exc} = 3.69(19)$ keV for the allowed β transition ^{111}In$(9/2^+) \rightarrow {}^{111}Cd(7/2^+)$.

One has the M1, M2, N1, N2, O1 and O2 (and possibly L2!) atomic-shell contributions at the endpoint:

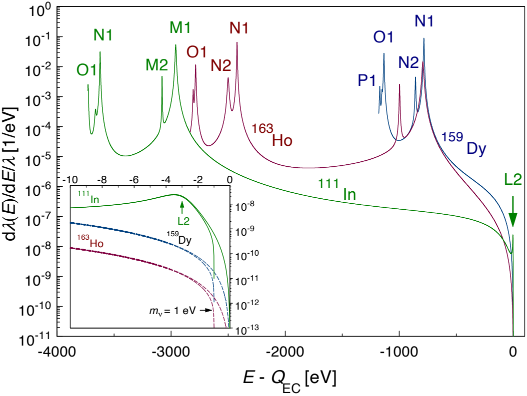

Still more information on the value of the weak couplings

These methods are now available:

For low momentum exchanges (g_A):

- Study half-lives of β decays (1^+ and 2^- states)
- Study half-lives of $2\nu\beta\beta$ decays (1^+ states)
- Study electron spectral shapes of β decays (J^π states)
- Study charge-exchange reactions
- Study double charge-exchange reactions

For high momentum exchanges like $0\nu\beta\beta$ decay ($g_{A,0\nu}$):

- Study charge-exchange reactions
- Study double charge-exchange reactions
- Study nuclear muon capture (J^π states)

Ordinary Muon Capture (OMC)

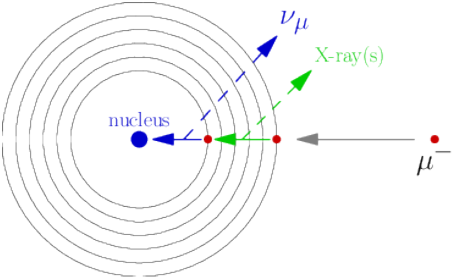

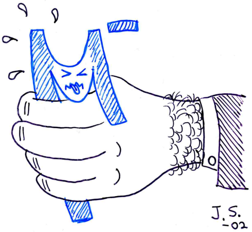

Nuclear muon capture:

OMC: ${}^{A}_{Z}X + \mu^- \rightarrow {}_{Z-1}^{\ \ A}Y + \nu_\mu$

Also:

Muon decay: $\mu^- \rightarrow e^- + \bar{\nu}_e + \nu_\mu$ $(\tau = 2.2\mu s)$

OMC probability $\sim Z^4$
(in Fe 91% are captured,
breakeven at $Z \sim 11$)

Ordinary muon capture (OMC) on ^{76}Se

$$^{76}\mathrm{Se} + \mu^- \rightarrow {}^{76}\mathrm{As} + \nu_\mu$$

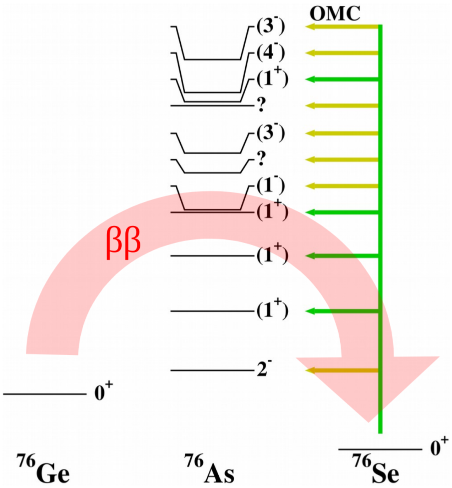

$$m_\mu c^2 \approx 105\,\mathrm{MeV}$$

- OMC and $0\nu\beta\beta$ operate in the $q \approx 100\,\mathrm{MeV}$ momentum-exchange region $\Rightarrow g_{\mathrm{A},0\nu}(J^\pi)$
- Induced currents (g_P!) are activated

Experiments:

RCNP, Osaka ; J-PARC MLF, Japan ; PSI, Villigen, Switzerland

The capture rate of OMC

The muon-capture rate (in units of 1/s) can be written as:

$$W = 2P \frac{2J_f + 1}{2J_i + 1} \Big(1 - \frac{q}{m_\mu + AM_N} \Big) q^2 \,,$$

where q is OMC Q-value (essentially the magnitude of the muon-neutrino momentum) and M_N the (average) nucleon mass. Here

$$P = \frac{1}{2} \sum_{\kappa u} \Big| g_{\rm V}(q^2) P^{(1)}_{\kappa u} + g_{\rm A}(q^2) P^{(2)}_{\kappa u} - \frac{g_{\rm V}(q^2)}{M_N} P^{(3)}_{\kappa u} + \sqrt{3} \frac{q}{2M_N} g_{\rm V}(q^2) P^{(4)}_{\kappa u}$$

$$+ \sqrt{6} \frac{q}{2M_N} \big(g_{\rm V}(q^2) - g_{\rm M}(q^2) \big) P^{(5)}_{\kappa u} - \frac{g_{\rm A}(q^2)}{M_N} P^{(6)}_{\kappa u} + \sqrt{\frac{1}{3}} \frac{q}{2M_N} \big(g_{\rm P}(q^2) - g_{\rm A}(q^2) \big) P^{(7)}_{\kappa u} \Big|^2$$

Compare with the inverse half-life of the $0\nu\beta\beta$ decay:

$$\Big(T^{(0\nu)}_{1/2} \Big)^{-1} = G_{0\nu} \Big(\frac{\langle m_\nu \rangle}{m_e} \Big)^2 \Big| [g_{\rm V}(q^2)]^2 M^{(0\nu)}_{\rm F} + [g_{\rm A}(q^2)]^2 M^{\rm (AA)}_{\rm GT} - \frac{q^2}{3M_N} g_{\rm A}(q^2) g_{\rm P}(q^2) M^{\rm (AP)}_{\rm GT}$$

$$+ \frac{q^4}{12M_N^2} [g_{\rm P}(q^2)]^2 M^{\rm (PP)}_{\rm GT} + \frac{q^2}{6M_N^2} [g_{\rm M}(q^2)]^2 M^{\rm (MM)}_{\rm GT} - [g_{\rm A}(q^2)]^2 M^{(0\nu)}_{\rm T} \Big|^2$$

OMC first suggested as an experimental probe for $0\nu\beta\beta$ matrix elements in:

Pioneering works:

M. Kortelainen and J. S., Ordinary muon capture as a probe of virtual transitions of $\beta\beta$ decay, *Europhysics Letters* **58** (2002) 666-672

M. Kortelainen and J. S., Microscopic study of muon-capture transitions in nuclei involved in double-beta-decay processes, *Nuclear Physics* **A 713** (2003) 501-521

M. Kortelainen and J. S., Nuclear muon capture as a powerful probe of double-beta decays in light nuclei, *Journal of Physics G: Nucl. Part. Phys.* **30** (2004) 2003-2018

Original theory from: M. Morita and A. Fujii, Theory of allowed and forbidden transitions in muon capture reactions, Phys. Rev. 118 (1960) 606.

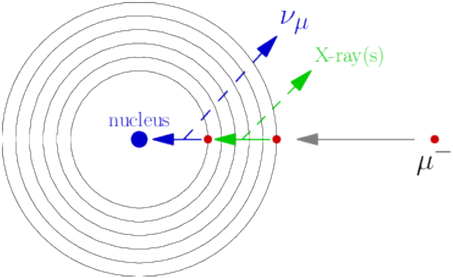

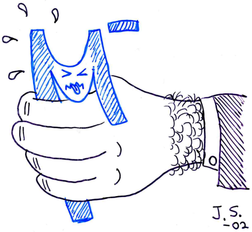

Nuclear muon capture:

$$\text{OMC: } {}^{A}_{Z}\mathrm{X} + \mu^- \rightarrow {}_{Z-1}^{\ \ A}\mathrm{Y} + \nu_\mu$$

Cumulative sums for the $0\nu\beta\beta$ matrix elements

NME calculated for the $0\nu\beta\beta$ decay of ^{48}Ca using the nuclear shell model

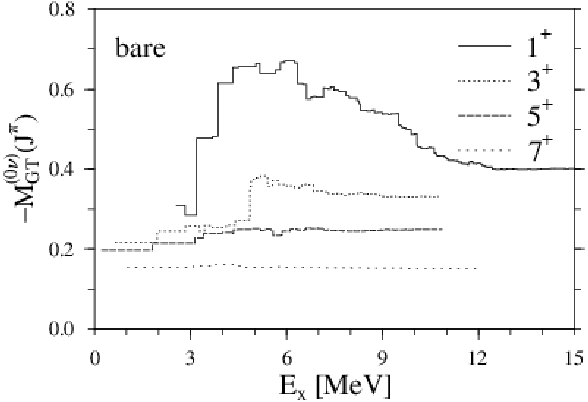

$$M^{(0\nu)} = \sum_{J^\pi} M^{(0\nu)}(J^\pi),$$

FPBP interaction in the pf shell:

$$\begin{aligned}
M(1^+) &= -0.402\\
M(2^+) &= -0.304\\
M(3^+) &= -0.332\\
M(4^+) &= -0.183\\
M(5^+) &= -0.249\\
M(6^+) &= -0.102\\
M(7^+) &= -0.151\\
\text{TOTAL} &= -1.723
\end{aligned}$$

OMC as a powerful tool to probe the $2\nu\beta\beta$ decay

$2\nu\beta\beta$ decay of ^{48}Ca and OMC on ^{48}Ti

$$M^{(2\nu)}_{\rm GT} = \sum_n \frac{M^{\rm L}_n(1^+_n) M^{\rm R}_n(1^+_n)}{D_n} = \sum_n M^{(2\nu)}(1^+_n),$$

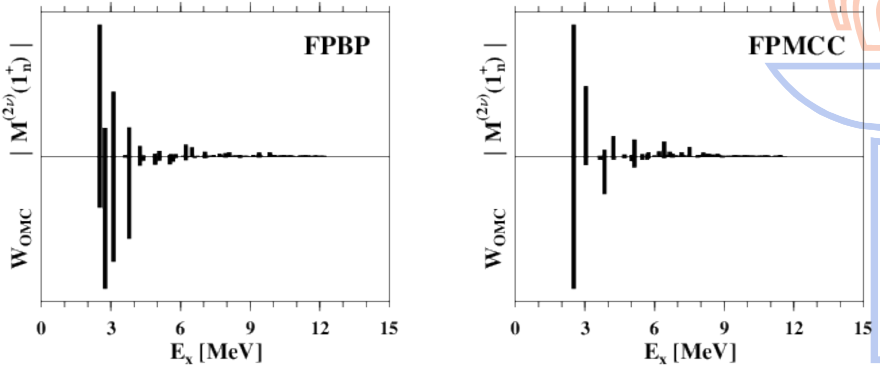

OMC as a tool to probe the $0\nu\beta\beta$ decay (Case of ^{48}Ca)

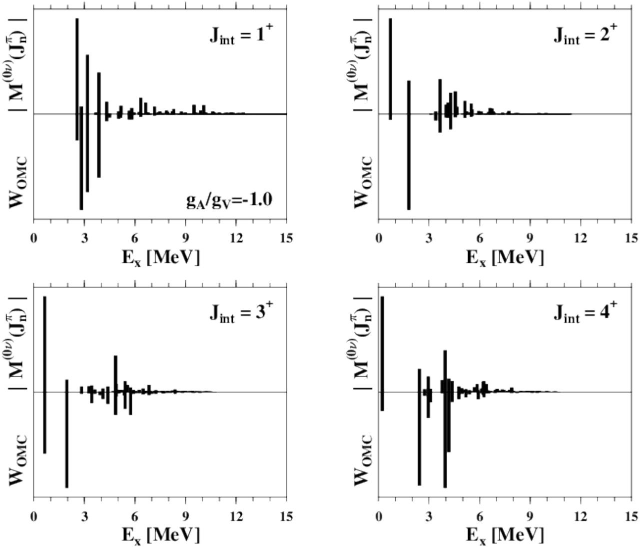

As before but with distributions of gaussian shape

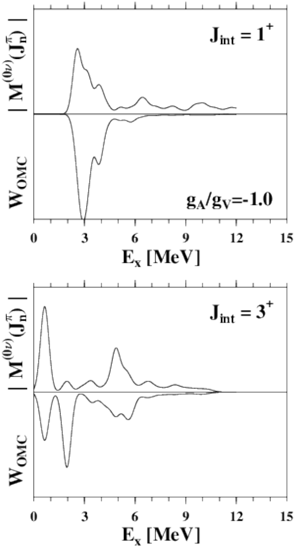

Recently: OMC in medium-heavy and heavy nuclei

There are and will be more data on:

PARTIAL CAPTURE RATES of OMC

and in particular:

OMC STRENGTH DISTRIBUTIONS

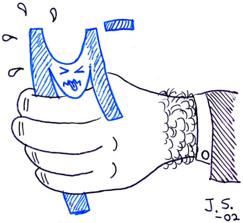

Now we need:

Large-basis (with Wood-Saxon single-particle energies) no-core pnQRPA calculations with realistic effective two-nucleon interactions.

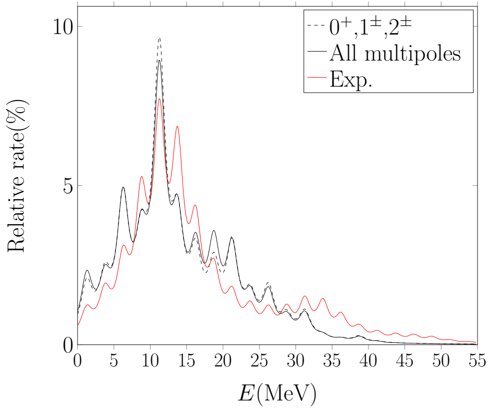

First evidence on OMC giant resonance:

L. Jokiniemi, J. S., H. Ejiri, I.H. Hashim, Pinning down the strength function for ordinary muon capture on ^{100}Mo, Phys. Lett. B 794 (2019) 143.

Experiments: MuSIC beam channel at RCNP (Research Center for Nuclear Physics), Osaka, Japan

D2 beam channel in J-PARC (Japan Proton Accelerator Research Complex) MLF, Ibaraki, Japan

Ongoing work: experiments at the μE4 beamline at PSI by The MONUMENT Collaboration

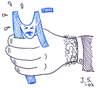

OMC strength functions: Transitions to various J^π states

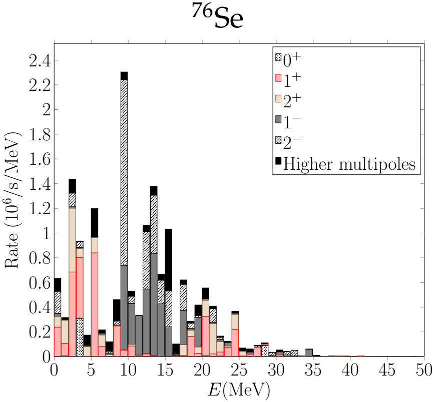

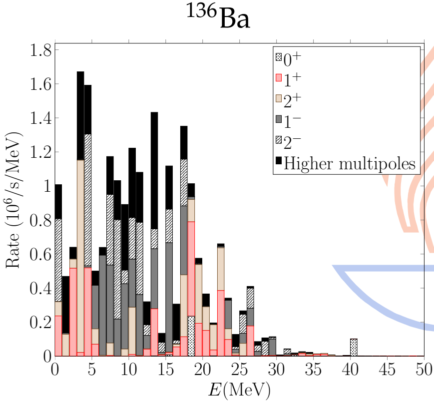

$0^+, 1^+$ and 2^+ strength: low-lying = $0\hbar\omega$ excitations, high-lying ($>$ 20 MeV) = $2\hbar\omega$ excitations

1^- and 2^- strength: low-lying "giant resonance" ($5-15$ MeV) = $1\hbar\omega$ excitations, high-lying ($>$ 25 MeV) = $3\hbar\omega$ excitations. The shape of the strength functions is not very sensitive to the values of g_A and g_P. (From: L. Jokiniemi and J. S., Muon-capture strength functions in intermediate nuclei of $0\nu\beta\beta$ decays, Phys. Rev. C 100 (2019) 014619)

Studied in: L. Jokiniemi and J. S., Comparative analysis of muon-capture and $0\nu\beta\beta$-decay matrix elements, Phys. Rev. C 102 (2020) 024303

VS.

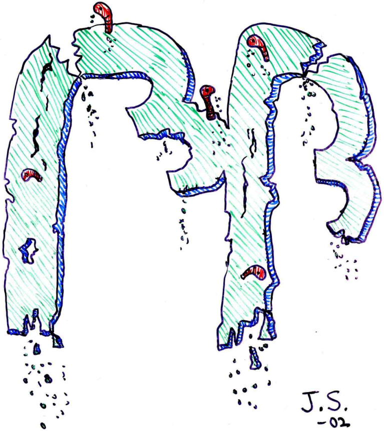

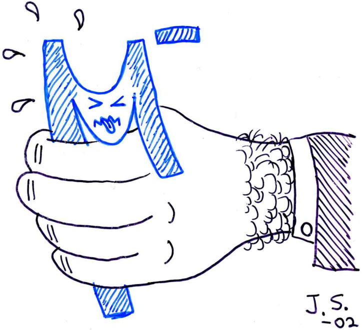

Comparative analysis between OMC rates and $0\nu\beta\beta$ NME for ^{76}Ge

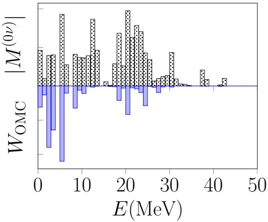

(a) $J^\pi = 1^+$

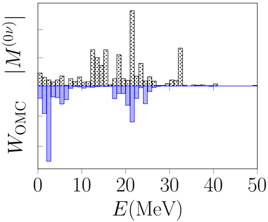

(b) $J^\pi = 2^+$

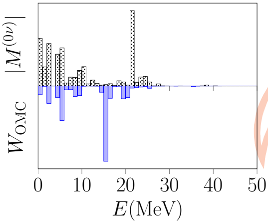

(c) $J^\pi = 3^+$

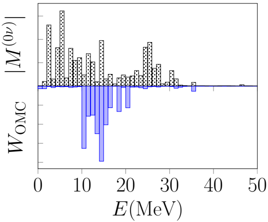

(d) $J^\pi = 1^-$

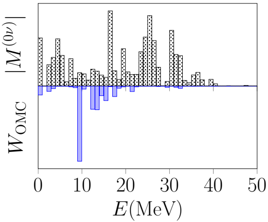

(e) $J^\pi = 2^-$

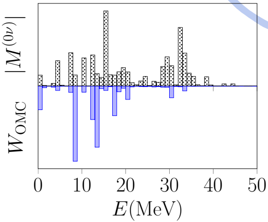

(f) $J^\pi = 3^-$

Comparative analysis between OMC rates and $0\nu\beta\beta$ NME for ^{136}Xe

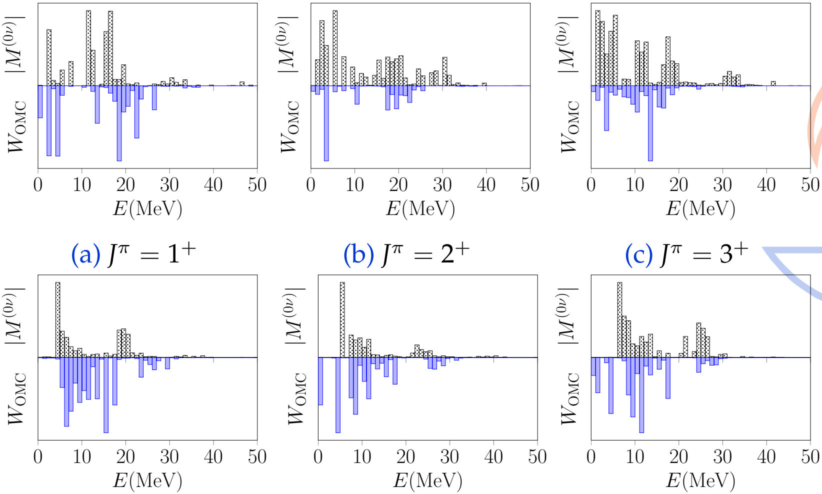

(a) $J^\pi = 1^+$ (b) $J^\pi = 2^+$ (c) $J^\pi = 3^+$

(d) $J^\pi = 1^-$ (e) $J^\pi = 2^-$ (f) $J^\pi = 3^-$

Cumulative relative (%) OMC rates and $0\nu\beta\beta$ NMEs

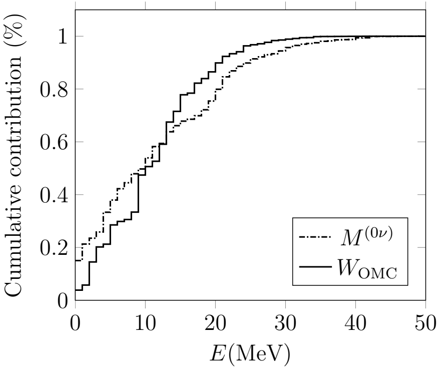

$A = 76$

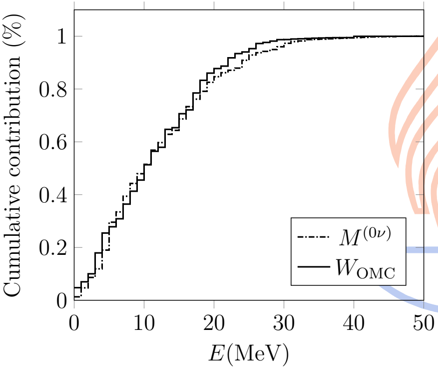

$A = 136$

From: L. Jokiniemi and J. S., Comparative analysis of muon-capture and $0\nu\beta\beta$-decay matrix elements, Phys. Rev. C 102 (2020) 024303

Comparison of the OMC and $0\nu\beta\beta$ multipole decompositions

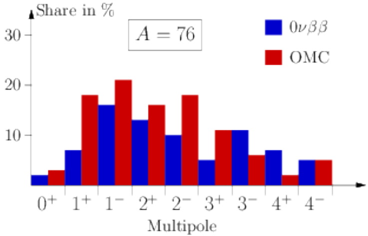

(a) OMC: 100%, $0\nu\beta\beta$: 76%

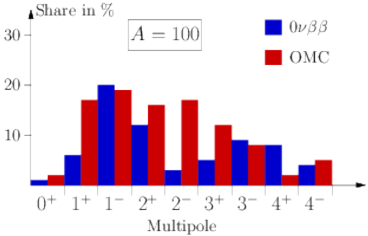

(b) OMC: 98%, $0\nu\beta\beta$: 68%

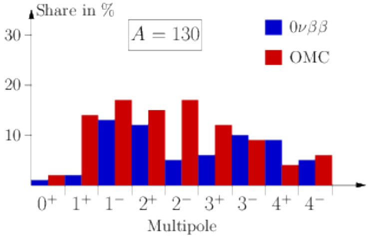

(c) OMC: 96%, $0\nu\beta\beta$: 63%

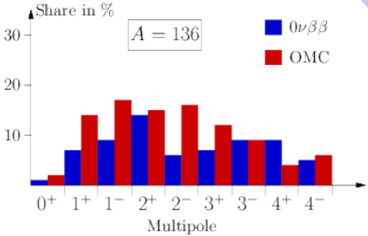

(d) OMC: 95%, $0\nu\beta\beta$: 67%

Recent and very recent work: OMC partial capture rates to individual final states

There are and will be more data on:

OMC CAPTURE RATES

to

INDIVIDUAL FINAL STATES

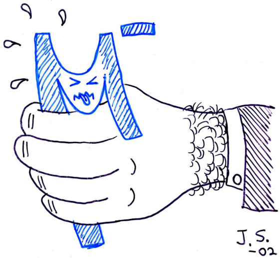

Now we can use:

pnQRPA theory, the nuclear shell model and ab initio methods

OMC to individual J^π states

OMC on ^{76}Se:

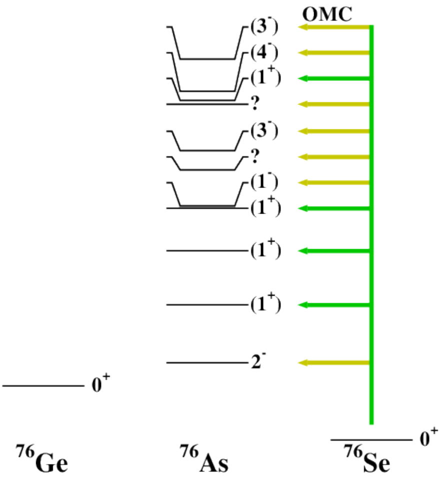

OMC on ^{76}Se: Rates to states J^π in ^{76}As below some 1 MeV: no-core large-basis pnQRPA calculation

$(g_V(0) = 1.0, g_A(0) = 0.8, g_P(0) = 7.0)$

J^π	Exp. (1/s)	Th. (1/s)
0^+	5120	414
1^+	218 240	236 595
1^-	31 360	28 991
2^+	120 960	114 016
2^-	145 920 + g.s.	177 802
3^+	60 160	55 355
3^-	53 120	34 836
4^+	-	2797
4^-	30 080	23 897

Data from: D. Zinatulina *et al.*, Phys. Rev. C 99 (2019) 024327

Calculation from: L. Jokiniemi and J.S., Phys. Rev. C 100 (2019) 014619

NEW: Add two-body meson-exchange currents

Quenching of the weak couplings by 2BC:

In addition to the one-body (weak nucleon) current (1BC) one can take into account the *meson exchanges* by adding (normal-ordered one-body part of) the two-body current (2BC) through the replacements:

$$g_A(q^2) \to (1 + \delta_a(q^2))g_A(q^2)\,,$$

$$g_P(q^2) \to \left(1 - \frac{q^2 + m_\pi^2}{q^2}\delta_a^P(q^2)\right)g_P(q^2)$$

See: M. Hoferichter *et al.*, Phys. Rev. D 102 (2020) 074018

NOTE: Does not account for deficiencies in the many-body framework!

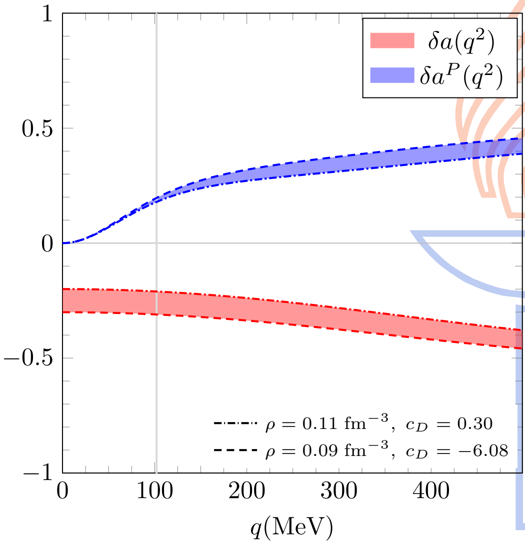

OMC on ^{12}C to individual J^π states in ^{12}B: 2BCs added

Shell-model calculated capture rates in units of 10^3 1/s, with $g_V(0) = 1.0$, $g_A(0) = 1.27$, $g_P(0)/g_A(0) = 6.8$ (PCAC, Goldberger-Treiman):

J^π	Exp.	Th.: 1BC	Th.: 1BC+2BC*
1^+_{gs}	$5.68^{+0.14}_{-0.23}$	6.48	3.98 – 4.45
2^+_1	$0.31^{+0.09}_{-0.07}$	0.42	0.30 – 0.32
2^+_2	$0.026^{+0.015}_{-0.011}$	0.011	0.008 – 0.009

* The spread comes from the spread in the assumed values of the EFT low-energy constants

Data from: Y. Abe *et al.*, Phys. Rev. C 93 (2016) 054608

Nuclear shell-model calculation from: L. Jokiniemi, T. Miyagi, S. R. Stroberg, J. D. Holt, J. Kotila and J.S., Phys. Rev. C 107 (2023) 014327

Recent work continues: OMC and double positron decays

NEW:

OMC

probing the

INITIAL BRANCH

of

DOUBLE BETA DECAY

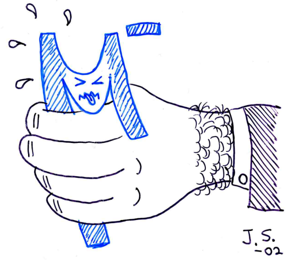

OMC and $0\nu\beta^+\beta^+$ decay of ^{106}Cd

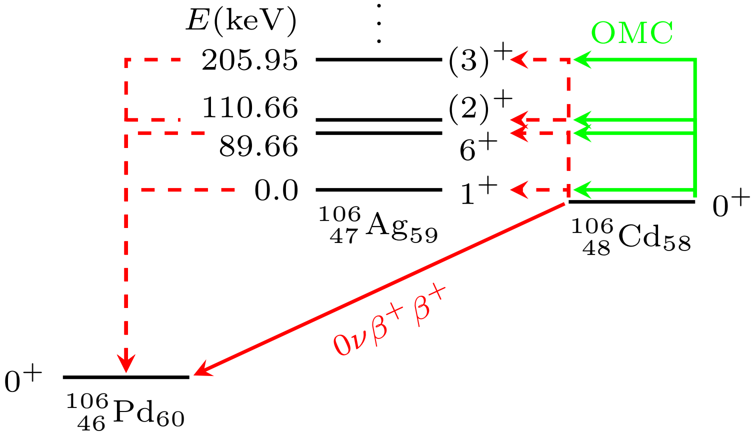

L. Jokiniemi, J.S. and J. Kotila, Comparative Analysis of nuclear matrix elements of $0\nu\beta^+\beta^+$ decay and muon capture in ^{106}Cd, Front. Phys. 9 (2021) 652536

OMC on ^{106}Cd: Muon orbital wave function

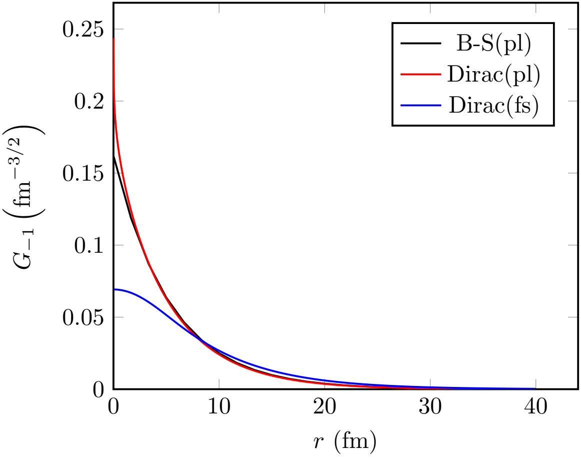

B-S: Bethe-Salpeter point-like nucleus approximation;

Dirac: Numerical solution of the Dirac equation;

pl: point-like nucleus;

fs: finite-size nucleus.

$$\mathrm{B-S}: \psi_\mu(\mathbf{r}) = \begin{pmatrix} -\mathrm{i}F_{-1}\chi_\mu \\ G_{-1}\chi_\mu \end{pmatrix}; \quad F_{-1} = -\sqrt{\frac{1-\gamma}{1+\gamma}}G_{-1}; \quad G_{-1} = \left(\frac{2Z}{a_0}\right)^{3/2}\sqrt{\frac{1+\gamma}{2\Gamma(2\gamma+1)}}\left(\frac{2Zr}{a_0}\right)^{\gamma-1}e^{-Zr/a_0}$$

^{106}Cd: OMC and $0\nu\beta^+\beta^+$ multipole decompositions

$0\nu\beta\beta$ decay

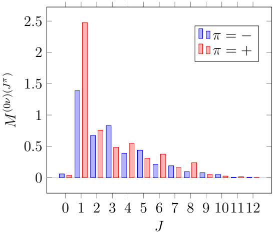

(a) Basis: 'Adj.'

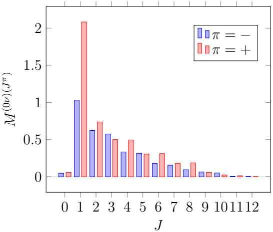

(b) Basis: 'WS'

OMC

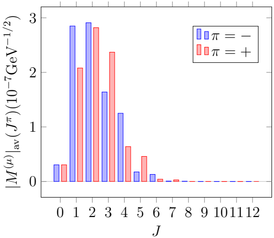

(a) Basis: 'Adj.'

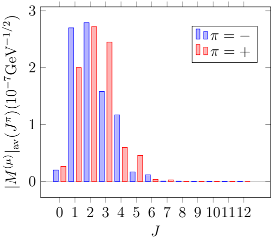

(b) Basis: 'WS'

Donald Henry Rumsfeld about "atomic effects" in CBS-NEWS:

Direct quotation:

'... there are known knowns. These are things we know that we know. There are known unknowns, that is to say, there are things that we now know we don't know. But there are also unknown unknowns, there are things we do not know we don't know.'